doi:10.26443/seismica.v3i2.1165

An exploration of potentially reversible controls on millennial-scale variations in the slip rate of seismogenic faults: Linking structural observations with variable earthquake recurrence patterns

T.K. Cawood [*1], **J.F. Dolan** [2]

[1]Natural Resources Canada, Geological Survey of Canada, Ottawa, Ontario, Canada, [2]Department of Earth Sciences, University of Southern California, Los Angeles, California, USA

Author contributions: *Conceptualization*: J.F. Dolan. *Investigation*: T.K. Cawood, J.F. Dolan. *Methodology*: T.K. Cawood. *Visualization*: T.K. Cawood. *Writing – original draft*: T.K. Cawood. *Writing – review & editing*: T.K. Cawood, J.F. Dolan.

Abstract Paleoseismic studies show that faults within a fault system may trade off slip over time, with mechanically complementary faults displaying alternating fast- and slow periods. Each of these periods spans multiple seismic cycles, and typically involves ~20 – 25m of slip. This suggests that the relative strength (or tendency to slip) of individual faults varies, over time and displacement scales larger than those of individual seismic cycles. The mechanisms responsible for these strength variations must: affect rocks in the strongest portion of the fault (the brittle-ductile transition) as this likely controls the overall slip rate of the fault; be reversible (or able to be counteracted) on a cyclical basis; provide a negative feedback that operates to change the fault from its current state; and have a measurable effect on fault strength over a time or length scale that corresponds to the observed fast and slow periods of fault slip. In this paper, we systematically explore 19 potential weakening and 11 potential strengthening mechanisms and evaluate them in light of these criteria. This analysis reveals a relatively small subset of mechanisms that could account for the observed behavior, leading us to suggest a possible model for fault strength evolution.

Production Editor: Gareth Funning
Handling Editor: Åke Fagereng
Copy & Layout Editor: Oliver Lamb

Signed reviewer(s): Luca Menegon, Ian Honsberger

Received: 10 Dec 2023
Accepted: 21 June 2024
Published: 22 July 2024

1 Introduction

Faults exhibit a wide range of behaviors, with some slipping at relatively constant rates (e.g. Pucci et al., 2008; Kozacıet al., 2009, 2011; Berryman et al., 2012; Grall et al., 2013; Kurt et al., 2013; Salisbury et al., 2018; Grant Ludwig et al., 2019), whereas others are characterized by wide variations in incremental slip rate (e.g., Weldon et al., 2004; Dolan et al., 2016, 2024; Zinke et al., 2017, 2019, 2021; Hatem et al., 2020; Griffin et al., 2022). These variations can span millennia, with multiple earthquake displacement pulses that span tens of meters of fault slip (e.g., Dolan et al., 2024). Interestingly, the constancy (or lack thereof) of fault slip through time correlates with the degree of relative structural complexity of the surrounding fault network. In an analysis of the incremental slip-rate behavior of major strike-slip fault systems around the world, Gauriau and Dolan (2021) demonstrated that structurally isolated faults that lie within relatively simple plate-boundary fault networks exhibit constant slip through time (Fig. 1). In marked contrast, faults that lie within structurally complex plate-boundary fault systems characterized by multiple, mechanically complementary faults, exhibit significantly more irregular behavior, with faults appearing to go through fast- and slow-slip periods that alternate as the faults within a system trade off slip in time and space (Gauriau and Dolan, 2021). In addition, a recent comparison of geodetic versus geologic rates suggests that the rates at which faults store and release strain energy varies through time, with major strike-slip faults in complex plate-boundary fault systems experiencing faster and slower periods of elastic strain accumulation consistent with accelerations and decelerations of their ductile roots (Gauriau and Dolan, 2024). These observations suggest that mechanically complementary faults within complex plate-boundary fault systems either (a) alternately strengthen and weaken through time, either in the upper crustal seismogenic part of the fault, or the ductile shear zone roots, with the weakest faults in the system slipping faster than their average rates, and/or (b) the rate of elastic strain accumulation on the mechanically complementary faults waxes and wanes such that faults are driven to slip faster or slower, depending on the rate of shearing in the ductile shear zone roots of the seismogenic faults (Dolan and Meade, 2017). As a result, fault systems may display fault-switching behavior, with the majority of the displacement accommodated by either one or another mechanically complementary fault, and alternating between them over time (Fig. 1).

An increasing number of incremental slip-rate records from major strike-slip faults suggest that

*Corresponding author: cawood.tk@gmail.com

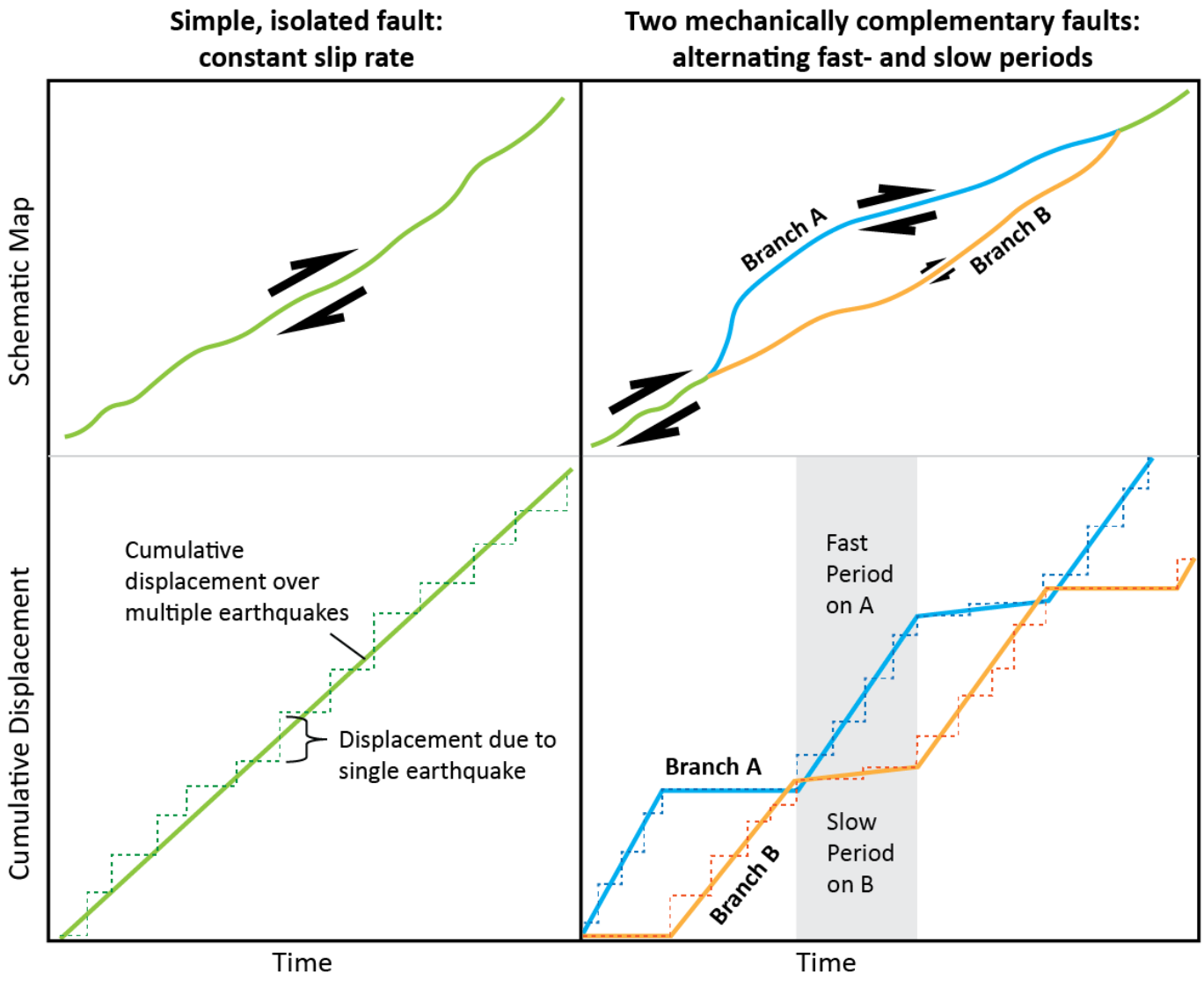

Figure 1 Schematic maps (top) and plots showing displacement over time (bottom), for a simple, isolated fault (left) compared to a fault system comprising two mechanically complementary branches (right).

displacements accommodated during periods of anomalously fast slip are on the order of a few tens of meters, with the duration of such fast intervals spanning from centuries to a few millennia (e.g., Weldon et al., 2004; Dolan et al., 2016, 2024; Zinke et al., 2017, 2019, 2021; Hatem et al., 2020; Griffin et al., 2022). For example, detailed event-by-event displacements documented for the past 15 surface ruptures at the Wrightwood site on the San Andreas fault (Weldon et al., 2004) suggest that the slip rate may have varied from as fast as ~90 mm/yr to as slow as ~15 mm/yr (see Dolan et al., 2016) over intervals spanning 5 – 6 earthquakes. Similarly, incremental slip rates documented during 4 – 6 earthquake clusters on the major strike-slip faults of the Marlborough fault system in northern South Island, New Zealand, reveal persistent patterns of alternating fast and slow/no slip rates spanning centuries to millennia in which the main plate-boundary strike-slip faults trade off slip in time and space (Zinke et al., 2017, 2019, 2021; Hatem et al., 2020; Dolan et al., 2024). The Garlock fault in southern California also exhibits wide variations in incremental slip rate ranging from ≥14 mm/yr during a cluster of 4 – 5 surface ruptures to as slow as ~3 mm/yr during intervening, millennia-long periods of slow slip (Dawson et al., 2003; Dolan et al., 2016; Dolan and Meade, 2017). Interestingly, in all of these examples the fast periods typically accommodate ~20-25 m of displacement (Weldon et al., 2004; Dolan et al., 2016, 2024; Zinke et al., 2017, 2019, 2021; Hatem et al., 2020; Fougere et al., 2024), suggesting that there may be something approaching complete stress drop in the upper crust, at least over these multiple-event periods of fast slip rate (Dolan et al., 2024).

The controls on these behaviors remain incompletely understood. Potential controlling mechanisms can be evaluated in light of four criteria that must be adhered to in order to explain the observed features. These mechanisms must:

1) Be reversible, or able to be counteracted by some other process, while keeping the P-T conditions constant (i.e., without appreciable exhumation or burial).
2) Operate to change the strength of the fault from its current state. i.e., the processes active during periods of relatively fast movement on the fault (when the fault is weak) must act to strengthen it, such that it

will begin to move more slowly, and those active during relatively slow periods (when the fault is strong) must act to weaken it, allowing it to speed up. **3) Operate on a timescale or length scale corresponding to ~20 – 25 m of displacement** (i.e., over multiple seismic cycles), consistent with paleoseismic studies (e.g., Weldon et al., 2004; Dolan et al., 2016, 2024; Zinke et al., 2017, 2019, 2021; Hatem et al., 2020). Depending on the specific slip rate, this key displacement may be achieved in centuries (e.g., the Wrightwood site on the San Andreas Fault, Weldon et al., 2004) or millennia (e.g., the Garlock Fault, Dolan et al., 2016). Strength variations related to the seismic cycle, such as transient deepening of the brittle-ductile transition (BDT) (e.g., Handy et al., 2007; King and Wesnousky, 2007), are unlikely to be the culprit unless they trigger or contribute to other, longer-term processes. The mechanism must therefore either be independent of the seismic cycle, or must have a cumulative effect that can build up over multiple cycles, and not an effect that dissipates during the interseismic period (like co-seismic frictional heating, e.g., Rowe and Griffith, 2015). **4) Affect rocks in the strongest part of the fault**, as their deformation rate will control the rate of ductile shear and thus the overall fault slip rate. This likely corresponds to the BDT, which coincides with a strength maximum between the downward-strengthening pressure (P)-dependent upper brittle crust, and the downward-weakening temperature (T)-dependent mid to lower crust (Sibson, 1977; Brace and Kohlstedt, 1980; Scholz, 1988; Behr and Platt, 2014).

Several mechanisms have been suggested to explain these behaviors. For example, Dolan et al. (2007) suggested that during fast-slip periods, the ductile shear zone roots of major seismogenic faults experience microstructural strain hardening as rates of intracrystalline dislocation tangling temporarily overwhelm recovery mechanisms, leading to a slowing of fault slip as the fault becomes more resistant to continued shear. When this occurs, other, mechanically complementary faults (i.e., those that accomplish part of the same overall work accommodated by the fault system) will be relatively weaker than the strain-hardened fault and will begin to slip faster than their average rates. In contrast, the mineral grains in the now-strain hardened ductile shear zone will gradually "anneal" (undergo recovery and removal of strain hardening effects). This will gradually re-weaken the fault such that it will be capable of undergoing another fast period. Alternatively, others have suggested that fluids may play a role in weakening faults. For example, Oskin et al. (2008) suggested that downward injection of fluids during large seismic ruptures on the upper crustal part of the fault could weaken the underlying ductile shear zone, causing it to slip faster. It is possible that such large fluid injections could have an effect that lasts for multiple seismic cycles.

In this study, we evaluate mechanisms described in the literature for weakening or strengthening faults, using the above four criteria to determine which mechanisms may be responsible for varying fault strength at the scale of the observed ~20 – 25 m of slip, and thus for driving the inferred slip trade-offs between mechanically complementary faults. We find that the processes most likely responsible for the inferred variations in fault strength include changes in the fluid content of the fault in the BDT; strengthening by hydrothermal cementation that is counteracted by the development of tectonic fabrics; microstructural strain hardening counteracted by grain-scale recovery; and the formation of active shear folds that are then passively transposed.

Note that we use the term "strength" to describe the level of differential stress required for deformation at a given strain rate (i.e., the resistance to shear). Thus, a weaker rock will deform at a lower stress than a stronger rock, at a constant strain rate (or will deform faster at a given stress). Note also that we focus predominantly on observations from strike-slip faults, which experience no appreciable exhumation or burial over the timescales involved. The term "fault" is used for the overall structure, comprising both the upper brittle fault and the lower ductile shear zone. And finally, although we discuss processes that occur within the brittle-ductile transition in the mid-crust, many of these mechanisms and resulting changes in shear-zone behavior will also operate on deeper parts of the ductile shear-zone roots.

2 Characteristics of faults in the BDT

General: The brittle-ductile transition (BDT) in a fault marks the change from pressure-dependent frictional behavior in the upper crust (characterized by brittle fault rocks that may slip seismically or aseismically, and that may be localized onto one or more discrete slip surfaces or distributed in meter-scale zones), to temperature- and rate-dependent viscous behavior in the mid- to lower crust (marked by predominantly aseismic crystal-plastic deformation and the development of ultramylonites and mylonites in shear zones of continuous, ductile deformation) (Sibson, 1977, 1982; Scholz, 1988; Handy et al., 2007). Rather than occurring at a single abrupt depth, this transition occurs over a depth range that is characterized by fluctuations in strain rate, deformation mechanisms, rheology, and fluid activity during the seismic cycle (Scholz, 1988; Rolandone et al., 2004; Handy et al., 2007; Frost et al., 2011; Maggi et al., 2014; Cao et al., 2017). This transition zone corresponds to the strongest portion of the crust (Sibson, 1982; Scholz, 1988; Handy et al., 2007; Bürgmann and Dresen, 2008; Behr and Platt, 2014), and possibly, in some tectonic settings, the strongest portion of the entire lithosphere (e.g., Bürgmann and Dresen, 2008).

In typical continental crust, the BDT occupies the ~15-20 km depth range (~300-450°C), although this varies with rock type, geothermal gradient, fluid content, and strain rate, among other factors (Sibson, 1977, 1982; Scholz, 1988; Rolandone et al., 2004; Singleton et al., 2020). For example, the deep crust (at ~600-700°C) can deform by alternating brittle- and ductile processes if it is particularly dry and strong (e.g., Hawemann et al., 2018). The typical depth of the BDT corresponds broadly to greenschist-facies conditions, such that the

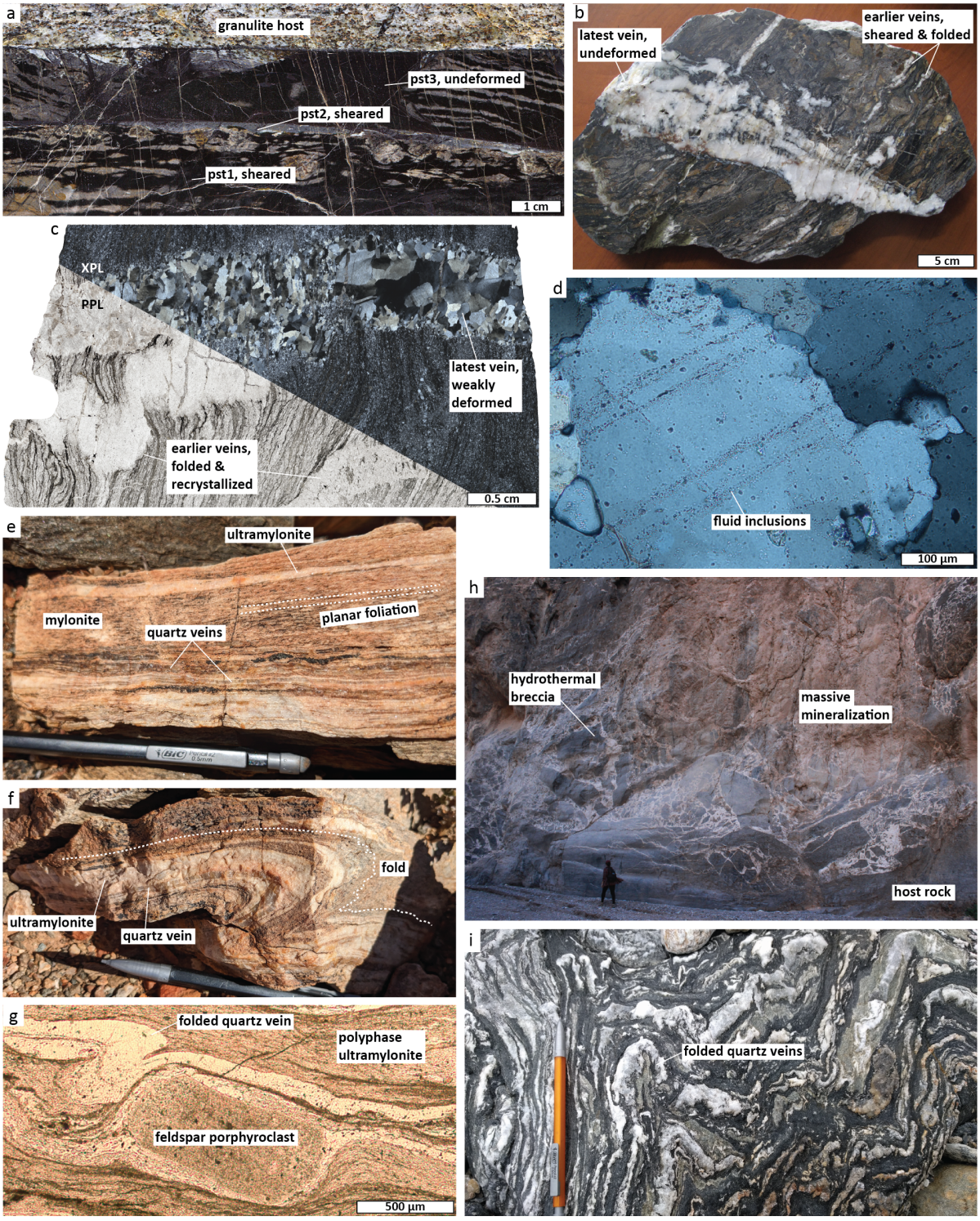

Figure 2 Photographs and photomicrographs showing key characteristics of the brittle-ductile transition, such as evidence for alternating periods of brittle deformation (pseudotachylites, quartz veins) and ductile deformation (folds, shearing, dynamic recrystallization); the presence of both planar fabrics and folds in a single shear zone; and significant hydrothermal cementation. a) Multiple generations of pseudotachylite (pst), with the older generations sheared. Photograph of a cut slab, courtesy of Friedrich Hawemann; see Hawemann et al. (2018, 2019) for details. b) Deformed polymict conglomerate cut by multiple generations of gold-bearing quartz veins, with earlier veins sheared and folded. Photograph courtesy of Ian Honsberger; see Honsberger et al. (2020) for details. c) Schist cut by multiple generations of quartz veins, with earlier veins folded and dynamically recrystallized, shown in plane- and cross polarized light (PPL and XPL). Thin section photomicrographs courtesy of Will Schmidt; see Schmidt and Platt (2022) for details. d) Planar arrays of fluid inclusions in quartz grains, representing healed microfractures, Cargo Muchacho Mountains, California. e-f) Planar (e) and folded (f) mylonitic fabric in a splay of the Pofadder Shear Zone, South Africa. g) Micro-scale fold affecting a dynamically recrystallized quartz vein adjacent to a rigid feldspar porphyroclast, Cuesta de Randolfo Mylonite Zone, Argentina. h) Hydrothermal breccia, Death Valley, California. i) Abundant folded quartz veins in mylonitic schist, Catalina Island, California.

BDT in felsic continental crust is associated with retrograde, hydrous chlorite and muscovite-bearing assemblages where fluid is available (forming phyllonites where retrogression is advanced), or deformed quartz and feldspar that remain stable if conditions remain dry (Imber et al., 2001; Spruzeniece and Piazolo, 2015; Cawood and Platt, 2021).

Co-seismic downward penetration of the BDT: Most earthquakes nucleate in the deeper part of the brittle upper crust, known as the "seismogenic zone" (Sibson, 1982). During the interseismic period, characterized by a low strain rate, shear zones at the BDT deform by viscous crystal-plastic mechanisms such as diffusion and dislocation creep, forming mylonites and ultramylonites and exhibiting relatively low strength (weak rheology). During large seismic events, however, earthquakes that nucleate in the brittle upper crust propagate downwards into the BDT (Scholz, 1988; Ellis and Stöckhert, 2004; Handy et al., 2007; King and Wesnousky, 2007). The associated high stresses and strain rates result in a transiently strong rheology and localized brittle failure within the BDT, transiently deepening the realm of seismic brittle faulting (Hearn and Bürgmann, 2005; Handy et al., 2007) by up to 4 km (Scholz, 1988) over a period of up to four years (Rolandone et al., 2004), and driving a period of postseismic creep at elevated rates (Ellis and Stöckhert, 2004; Campbell and Menegon, 2019).

Mutually overprinting brittle and ductile structures: The BDT is thus characterized by mutually overprinting ductile structures formed during the interseismic periods (such as mylonites, ultramylonites, and folds), and features formed by co-seismic brittle failure, such as discrete fault surfaces, cataclasites, quartz veins, and pseudotachylites (Fig. 2; Scholz, 1988; Handy et al., 2007; Frost et al., 2011; Price et al., 2012; Wintsch and Yeh, 2013; Melosh et al., 2018; Sullivan and O'Hara, 2021).

Fabrics: The fabric of rock within the BDT may thus vary from homogenous mylonite, ultramylonite, or cataclasite with a well-developed tectonic foliation (schistosity, cleavage), to a complex zone of overprinting ductile foliations, brittle structures, and veins. This fabric may vary from planar to wavy or even highly folded, with spatial variations within a single shear zone commonly observed (e.g., the Pofadder Shear Zone, Melosh et al., 2018).

Fluids and hydrothermal mineralization: Finally, the rock within the BDT may remain relatively unaltered, or it may record significant fluid flow in the form of metasomatic alteration (Putnis and Austrheim, 2010; Spruzeniece and Piazolo, 2015), cemented zones (Callahan et al., 2020), or abundant hydrothermal veins (Fig. 2b,i; Frost et al., 2011) or breccias (Fig. 2h). For example, many shear-hosted orogenic gold deposits form in the BDT (Sibson et al., 1988; Goldfarb et al., 2005), and are characterized by abundant gold-bearing quartz veins that may be tens of meters in width, with vein sets extending several kilometers vertically and laterally (Goldfarb et al., 2005).

3 Potential weakening mechanisms

Various processes can lead to weakening of a shear zone, decreasing the stress required to drive deformation or allowing a faster deformation rate at a constant imposed stress. If such processes are not reversed or counteracted by a strengthening process, they will lead to strain localization and the progressive narrowing of the shear zone (e.g., Cawood and Platt, 2021). In this paper, we number the weakening mechanisms most discussed in the literature as W1-W19; these are summarized in Table 1 and briefly described here, with additional details in Supplementary Table S1.

3.1 Adding fluids

The addition of fluids to the BDT can lead to weakening by several mechanisms, some of which can be reversed or counteracted, whereas others are likely to be unidirectional:

Adding fluids can enable **(W1) reaction weakening**, the replacement of stronger phases such as feldspar or amphibole by weaker, hydrous, retrograde phases like muscovite and chlorite (Imber et al., 2001; Wintsch and Yeh, 2013; Spruzeniece and Piazolo, 2015; Cao et al., 2017; Cawood and Platt, 2021). The fine grain size and unstrained nature of reaction products may further enhance weakening (White and Knipe, 1978). However, this weakening effect is permanent unless the rocks are subjected to higher pressure-temperature conditions, either through burial or the input of magmatic or other heat, resulting in metamorphic devolatilization and the prograde re-growth of stronger phases. As highlighted in Section 1, the feasibility of potential weakening mechanisms can be evaluated using four criteria. Burial violates the first of these, namely, that the mechanism be active at a constant depth, and although prograde contact metamorphism adjacent to intruding magma may occur in some cases, it is unlikely to repeat cyclically. Co-seismic frictional heating or viscous shear heating may locally elevate temperature, driving local devolatilization of carbonates or dehydration of hydrous minerals (Leloup et al., 1999; Rowe and Griffith, 2015; Mako and Caddick, 2018), but is unlikely to drive shear zone-wide reversal of retrogressive reaction weakening.

Fluids can also lead to significant **(W2) hydrolytic weakening** if they are present within mineral grains (Griggs and Blacic, 1965; Kronenberg and Wolf, 1990), and the presence of such intracrystalline or intragranular water has been experimentally shown to increase rates of dynamic recrystallization in quartz (Palazzin et al., 2018). Early studies on quartz attributed hydrolytic weakening to intracrystalline OH- defects that weaken the bonds in the quartz crystal lattice by hydrolysis and thus enable faster plastic deformation (Griggs and Blacic, 1965; Kronenberg and Tullis, 1984). Subsequent experimental and natural studies, however, suggest that significant weakening is instead caused by water present as fluid inclusions and molecular clusters (e.g., Kronenberg et al., 1986, 2020), which weaken the grains by generating dislocations within the crystal lat-

Table 1 Weakening mechanisms

	Potential Weakening Mechanisms	Description	1. Reversible at constant depth?	2. Change shear zone strength from its current state?	3. Effective over ~20 – 25 m/500 – 5,000 year scales?	4. Active in BDT?
	Add Water:					
W1	**Reaction weakening**	Stronger phase replaced by weaker hydrous phase	X	~	~	✓
W2	**Hydrolytic weakening**	Intragranular OH- weakens lattice, and/or fluid inclusions & molecular water weaken grains by generating dislocations	✓	✓	~	✓
W3	**Fluid-enhanced diffusion**	Intergranular fluids enable faster diffusion	✓	~	~	✓
W4	**Fluid overpressure & hydraulic embrittlement**	Increased pore fluid pressure decreases the effective normal stress	✓	✓	X	✓
W5	**Fluid-filled porosity**	Fluid-filled spaces act as a weak phase within a rock	✓	~	~	✓
	Grainsize decrease:	Enables faster deformation by grainsize-sensitive mechanisms or triggers a deformation mechanism switch				
W6	**Cataclastic grain-size decrease**	Forms finer-grained grain & rock fragments	✓	X	~	✓
W7	**Pseudotachylite formation**	Frictional melting creates ultra-fine grained/glassy products	✓	X	~	✓
W8	**Dynamic recrystallization**	Creates new, smaller grains	✓	X	~	✓
W9	**Fine-grained reaction products**	Replacement of coarse minerals with new, finer grained minerals	X	~	~	✓
	Microstructural evolution:					
W10	**Phase mixing**	Maintains a smaller grainsize by pinning	~	X	~	✓
W11	**Fabric development**	Anisotropic rock is weaker (in certain directions) than comparable massive rock	~	~	~	✓
W12	**Viscous aniostropy**	Forms a new CPO, with grains aligned for slip on easiest slip system	~	X	~	✓
W13	**Interconnected weak layers**	Decrease overall strength	~	X	~	✓
W14	**Crystal lattice recovery**	Counteracts work hardening of grains	✓	✓	~	✓
	Macroscopic geometric evolution:					
W15	**Fault maturation**	Smoothing of geometric irregularities with cumulative slip	X	X	~	✓
W16	**Anastomosing networks**	Linkage of weak lenses or strands within a fault zone, to form large-scale interconnected weak layers	X	X	~	✓
W17	**Rotational weakening**	Progressive rotation of dominant anisotropy towards the shear plane	✓	✓	✓	✓
	Thermal weakening:	Heating can weaken rock by creating melt, driving the release of fluids or volatiles, or enhancing crystal plastic deformation				
W18	**Co-seismic frictional heating**	Heat released by fast frictional sliding during seismic rupture	✓	X	X	✓
W19	**Co-seismic frictional heating**	Heat released by fast frictional sliding during seismic rupture	✓	X	~	✓

✓= yes, ~ = possibly, X = no

tice (Stünitz et al., 2017). This weakening is most effective if the fluid inclusions are small, such as after they have been modified and decrepitated (broken) during crystal plastic deformation. As such, quartz with the same fluid content but in fewer, larger inclusions tends to be stronger (Stünitz et al., 2017). Recent studies on quartz deformed by nanoindentation found that water had no measurable weakening effect at the experimental conditions, and suggested that hydrolytic weakening may only be important at relatively higher temperatures, lower stress or strain rate conditions, and/or in strain-free water-rich grains (Strozewski et al., 2021; Ceccato et al., 2022).

Intergranular fluids, present in pores, cracks, microcracks, or along grain boundaries, can also **(W3) enhance diffusion** and thus deformation by mechanisms such as dissolution-precipitation creep and diffusion-assisted grain boundary sliding. Such intergranular fluids can also enhance grain boundary mobility and thus dynamic recrystallization by grain boundary migration (Mancktelow and Pennacchioni, 2004; Pongrac et al., 2022).

Furthermore, the accumulation of intergranular fluids and resulting **(W4) fluid overpressure** decreases the effective normal stress and thus makes the rock more susceptible to brittle failure (hydraulic embrittlement). While technically this reflects a strengthening of the rock in that it enhances brittle failure over ductile flow, we consider fluid overpressurization a weakening mechanism here because it may enable significant displacement of otherwise slowly deforming rock. Note that hydraulic fractures can be relatively small, and do not necessarily have to link up with surface ruptures.

In addition, although the pressure of pore fluids has long been recognized as significant in reducing effective normal stress, recent work suggests that the fluid volume fraction and topology or geometry of the fluid-filled space is also important (Okazaki et al., 2021). This **(W5) fluid-filled porosity** acts as inclusions of a weak phase within a stronger rock. Such weak phases reduce the overall strength of the rock (e.g., Handy, 1994).

All these fluid-related weakening mechanisms may be active in the BDT, satisfying Criterion 4. However, (W1) reaction weakening violates Criterion 1 as it is unlikely to be reversed or counteracted at a constant depth. The rate at which fluid overpressure (W4) builds up depends on a variety of factors (such as the rates of fluid production and migration), but such fluid overpressure is inherently cyclic and typically linked to the seismic cycle, in that the resulting brittle failure (hydrofracturing) results in a sudden pressure decrease, removing the mechanism of weakening (the fault valve model of Sibson et al., 1988). Fluid overpressure thus violates Criterion 3 as it fluctuates on a much shorter timescale (that of the seismic cycle). The remaining mechanisms (W2 hydrolytic weakening, W3 enhanced diffusion, and W5 fluid-filled porosity) may be counteracted if the fluids are somehow removed from the crystal lattices or intergranular spaces, respectively, and may act over the required 20 – 25 m-scale, but this will be determined by the rate at which fluids enter the BDT, the rate at which the weakening mechanism itself acts, and the rate at which the fluids are expelled.

3.2 Grain size decrease

A grain size decrease can weaken rocks that are deforming by a grain size-sensitive mechanism (such as diffusion creep or diffusion-enhanced grain boundary sliding; e.g., Rutter and Brodie, 1988; Stünitz and Tullis, 2000; Platt and Behr, 2011; Okudaira et al., 2017; Mulyukova and Bercovici, 2019), in which smaller grain sizes will enable deformation at lower stress at a given strain rate. In rocks that are deforming by a grain size-insensitive mechanism, like dislocation creep, a grain size decrease can trigger a switch to a grain size-sensitive mechanism, and thereby induce weakening (White, 1977; Platt and Behr, 2011). Various processes can cause grain size decrease:

Transient brittle failure can result in **(W6) cataclastic grain size decrease** (e.g., Song et al., 2020), as well as the formation of glassy and/or ultra-fine grained **(W7) pseudotachylites** (Fig. 2a) during highly localized frictional melting, which at mid-crustal conditions are typically weaker than their wallrocks and will favour strain localization (Price et al., 2012; Kirkpatrick and Rowe, 2013; Campbell and Menegon, 2019; Hawemann et al., 2019). Such brittle failure may result from deep penetration of large earthquake ruptures or fluid overpressure resulting in hydraulic fracturing, and thus occurs over a very short duration (on the scale of seconds, Fig. 3), and likely repeats on the scale of the earthquake cycle. Transient high stresses (and resulting rapid brittle failures) can also develop in the middle and lower crust due to heterogeneous deformation within otherwise-ductile shear zones (Hawemann et al., 2019). These processes are at least partially reversible, because the fine grain size (and typically hydrous nature) developed during co-seismic brittle failure makes pseudotachylites particularly susceptible to grain growth by static recrystallization (Kirkpatrick and Rowe, 2013). Pseudotachylites also concentrate hydrous phases (W1), create interconnected weak layers (W13), and localize interseismic mylonitization (W8), and the accumulation of thick zones of variably deformed pseudotachylite within the BDT (as documented in the Norumbega Shear Zone, Maine) can result in persistent long-term weakening (Price et al., 2012). This long-term weakening mechanism will be most effective during periods of fast slip and deep rupture penetration, and thus acts to enhance weakening of the already weakened shear zone. It thus violates Criterion 2, and although potentially important in the long-term strength evolution of shear zones, it is not one of the mechanisms we seek.

(W8) Dynamic recrystallization and the formation of **(W9) fine-grained reaction products** can also lead to a grain size decrease (White, 1977; Platt and Behr, 2011; Cawood and Platt, 2021), and can occur during interseismic crystal plastic deformation. These mechanisms of grain size decrease can be counteracted by grain growth under different boundary conditions, such as higher temperatures, slower strain rates (decreased imposed stress), or more hydrous conditions (e.g., Platt and Behr, 2011). If the boundary conditions remain

constant, grain growth is thus unlikely to trigger fault strengthening. If, however, another mechanism independently strengthens the fault, the resulting decreased strain rate may enable grain growth, which could then contribute to additional fault strengthening.

3.3 Fabric development and microstructural evolution

Several other weakening processes act at the micro-scale, controlled by changes in the rock microstructure:

Dynamic recrystallization and hydration reactions both enable **(W10) phase mixing**, which then enhances and maintains a grain size decrease (and thus weakening) by Zener pinning (Platt, 2015; Mulyukova and Bercovici, 2019).

(W11) Foliation development is a typical result of deformation. The formation of a tectonic foliation (schistosity or cleavage) in a previously massive or anisotropic rock significantly weakens the bulk rheology (Jordan, 1988). Foliation development occurs by several mechanisms, including the mechanical rotation of tabular or platy minerals (such as micas, amphiboles, or clays) into a preferred alignment; crystal plastic deformation and dynamic recrystallization of existing grains to form a shape fabric (by dislocation or diffusion creep); recrystallization and growth of oriented new grains; and the development of a differentiated syn-deformation metamorphic fabric, such as alternating quartz- and mica-rich layers (Passchier and Trouw, 2005). Furthermore, the development of a shape fabric can cause weakening through **(W12) viscous anisotropy**, or the development of a new crystallographic preferred orientation (CPO) aligned for slip on the easiest slip system for the specific PT conditions (Muto et al., 2011; Hansen et al., 2012).

The development of **(W13) interconnected weak layers** (IWLs) of a relatively weaker phase, such as mica or a mixture of fine-grained minerals, leads to a decrease in the bulk strength of the rock (Handy, 1994; Cole et al., 2007; Montési, 2013; Wintsch and Yeh, 2013). Such IWLs can form due to dissolution-precipitation creep; grain size reduction and grain boundary sliding; disaggregation of coarse-grained micas; hydrous retrograde replacement of feldspar or other phases by weaker micas; phase segregation due to crenulation cleavage development; or even due to progressive deformation within pseudotachylite layers (Passchier and Trouw, 2005; Price et al., 2012; Wintsch and Yeh, 2013; Platt, 2015).

Fabric development and microstructural evolution are predominantly unidirectional processes, with progressive deformation (at the same PT conditions) simply enhancing them. However, these processes may be counteracted by hydrothermal cementation or the emplacement of abundant veins, which will destroy the existing rock fabric and microstructure.

(W14) Recovery refers to the removal of defects from the crystal lattice of mineral grains (White, 1977), resulting in strain-free grains and thus counteracting work hardening. Recovery involves the replacement of highly strained grains (or portions of grains) with strain-free grains via dynamic recrystallization, driven by the reduction in internal strain energy (dislocation density). Note that W8 refers specifically to the grain-size decrease that results from dynamic recrystallization, whereas W14 refers to the creation of unstrained, weaker grains by dynamic recrystallization during recovery.

At higher stresses and/or lower temperatures, dynamic recrystallization occurs by bulge nucleation (BLG), whereby grains with low dislocation density grow at the expense of adjacent work-hardened grains (Tullis and Yund, 1985; Hirth and Tullis, 1992). At sufficiently high temperatures, dislocation climb allows dislocation tangles to be bypassed, allowing dislocations to be shifted into lower energy subgrain boundaries and dynamic recrystallization to occur by subgrain rotation (SGR) (White, 1977; Passchier and Trouw, 2005). Dislocation climb (and thus recovery and dynamic recrystallization) is enhanced by higher temperatures and the presence of water (Tullis and Yund, 1989; Palazzin et al., 2018; Pongrac et al., 2022).

3.4 Macroscopic geometric evolution

Several macro-scale processes may also lead to weakening, by changing the geometry of the shear zone:

(W15) Fault maturation sees faults becoming progressively smoother with increasing displacement, developing a simpler, straighter geometry as irregularities are destroyed during progressive slip (Wesnousky, 1988; Hatem et al., 2017). This is inherently a unidirectional process.

The linkage of faults or weak lenses within shear zones into **(W16) anastomosing networks** (effectively large-scale IWLs) decreases the overall strength of the fault system/domain (Handy et al., 2007). However, as for the formation of micro-scale IWLs and fault maturation, this is effectively a unidirectional process that is not typically reversed or counteracted.

Rocks may contain mechanical anisotropies in the form of pre-existing foliations, compositional banding, or sedimentary layering. **(W17) Rotational weakening** entails the progressive rotation of the dominant mechanical anisotropy towards the macroscopic shear plane, causing folds to become isoclinal and the dominant anisotropy to become transposed into the shear plane, with a resultant reduction in the bulk rock strength (Cobbold, 1977). Rotational weakening is reversible, in that it may be counteracted by the development of folds during ongoing shearing, which require only small irregularities to nucleate and grow (Melosh et al., 2018).

3.5 Heating

Finally, **(W18) co-seismic frictional heating** and **(W19) viscous shear heating** may weaken the rocks of the BDT, by raising the T and thus creating weak melt, releasing fluids or other volatiles by mineral devolatilization, or enhancing thermally activated crystal plastic deformation mechanisms (Leloup et al., 1999; Rowe and Griffith, 2015; Mako and Caddick, 2018). Both require

fast, highly localized strain, and will thus be most effective in the uppermost BDT, or during deep penetration of large earthquake ruptures. However, both are unlikely to be significant during the interseismic period, and the effectiveness of viscous shear heating in natural shear zones has been questioned (Platt, 2015; Mako and Caddick, 2018). Both frictional and viscous shear heating will be most significant during large, deeply penetrating earthquake ruptures, which are most common during periods of faster fault slip. If frictional and/or viscous shear heating have a noticeable effect on shear zone strength, it will be to weaken the shear zone during the period when it is thus already relatively weak and fast (thereby violating Criterion 2). They are therefore unlikely to be some of the mechanisms we are searching for, and indeed, any mechanism we identify that can strengthen a shear zone during a period of fast slip must work against the effects of frictional and viscous shear heating.

4 Potential strengthening mechanisms

Several processes may strengthen a shear zone. If these are not reversed or counteracted, they will lead to broadening of the shear zone, as the actively deforming portion is abandoned in favor of adjacent, weaker rock (Finch et al., 2016). Alternatively, the shear zone may be abandoned entirely, and slip will be transferred onto a nearby structure or a new shear zone formed in nearby weaker, undeformed rock (e.g., Woodcock et al., 2007). Here, we briefly describe the most common strengthening mechanisms (termed S1 – S11, see also Table 2 and Supplementary Table S2).

4.1 Dehydration

Dehydration of the shear zone can strengthen it, as the various weakening effects of fluids are removed (Finch et al., 2016). The **(S1) expulsion of intracrystalline water** will decrease the effects of hydrolytic weakening on minerals deforming by crystal plasticity. Dynamic recrystallization by subgrain rotation or grain boundary migration can expel water hosted by fluid inclusions and hydrous defects from quartz grains (Palazzin et al., 2018; Kronenberg et al., 2020). Furthermore, drastic heating during seismic events can drive dehydration and devolatilization, converting for example limestone to stronger dolostone (Rowe and Griffith, 2015), and even less-drastic frictional or viscous shear heating may drive water expulsion.

The **(S2) removal of intergranular fluids** will lead to slower diffusion and thus slower deformation by diffusion-dominated processes, even in fine-grained shear zone rocks. Removal of intergranular fluid will also lower the pore fluid pressure, reducing the weakening effect of fluid-filled porosity, and preventing hydrofracturing.

4.2 Grain size increase

Grain growth can strengthen rock as diffusion-dominated deformation mechanisms become slower, or as the dominant deformation mechanism switches from diffusion- to dislocation creep. Several processes can lead to grain size increase:

(S3) Annealing or static recrystallization of grains can cause grain growth. For dynamically recrystallized grains, this requires that the imposed strain rate slows sufficiently, or that deformation pauses completely, while the rock is still at a relatively elevated T (Platt and Behr, 2011). Thus, static recrystallization is unlikely to be the initial cause of strengthening and resulting strain rate decrease; however, if another mechanism initially decreases the strain rate to below some threshold, grain growth by static recrystallization may further strengthen the rock. Rocks that achieved a fine grain size during seismic events (such as pseudotachylites or cataclasites) are particularly susceptible to grain growth by static recrystallization during interseismic periods, due to their very fine grain sizes and possible greater water contents (Kirkpatrick and Rowe, 2013). Note, however, that such grain growth by static recrystallization is likely only effective in monomineralic rocks. Many ultramylonites are instead polymineralic, and grain growth will be inhibited by second-phase pinning (see W10).

In addition, existing grains may grow during (typically prograde) **(S4) metamorphic reactions**. However, this requires a change in PT conditions, violating Criterion 1, and thus cannot be our culprit.

4.3 Growth or precipitation of new phases

The growth of new mineral phases can also strengthen the shear zone, if the new phases are relatively stronger, coarser grained, or more massive than the pre-existing material:

(S5) Reaction hardening refers to the growth of new, stronger phases during metamorphic reactions, such as feldspar at the expense of micas. Most such reactions are prograde, requiring an increase in PT conditions, making them unsuitable candidates. New, stronger minerals may, however, also be formed by retrograde reactions (which occur at constant PT conditions with the addition of water) or metasomatic reactions (which require an externally derived fluid in disequilibrium with the bulk rock; Putnis and Austrheim, 2010). For example, Maggi et al. (2014) showed that fluid flow within a shear zone in granodiorite drove the growth of new, relatively strong K-feldspar within previously weakened, altered, mica-rich phyllonites.

Without the involvement of fluids, reaction hardening is unlikely to be reversible, as the reaction products will remain stable unless the PT conditions change. With the involvement of externally-derived fluids, however, changes in the fluid chemistry and/or fluid:rock interaction can drive changes in the stability of different minerals, variably causing reaction weakening or reaction hardening (Maggi et al., 2014).

(S6) Cementation, the precipitation of new hydrothermal phases such as quartz or carbonate, can

Table 2 Strengthening mechanisms

	Potential Strengthening Mechanisms	Description	1. Reversible at constant depth?	2. Change shear zone strength from its current state?	3. Effective over ~20 – 25 m/500 – 5,000 year scales?	4. Active in BDT?
	Remove Water:					
S1	**Expulsion of intracrystalline water**	Removes effects of hydrolytic weakening	✓	✓	~	✓
S2	**Expulsion of intergranular fluids**	Removes effects of fluid-enhanced diffusion, fluid overpressure, and fluid-filled porosity	✓	~	~	✓
	Grainsize increase:	Larger grains deform more slowly by grain size-sensitive mechanisms				
S3	**Annealing (static recrystallization)**	Grain growth at lower stresses/slower strain rates	✓	X	~	✓
S4	**Metamorphic grain growth**	Finer-grained phases replaced by coarser minerals	X	~	~	~
	Growth of new phases:	New phases may be more competent, coarser grained, and/or destroy existing fabrics & microstructures				
S5	**Reaction hardening**	Weaker phases replaced by stronger ones	X	~	~	~
S6	**Cementation**	Precipitation of new phases by hydrothermal fluids	✓	✓	✓	✓
	Other microstructural changes:					
S7	**Strain hardening**	Dislocations accumulate & become tangled	✓	✓	~	✓
S8	**Anisotropy rotation (geometric strengthening)**	Existing anisotropies become less suitably oriented for slip	✓	~	~	✓
S9	**Dissolution-precipitation**	Material dissolved and re-precipitated elsewhere	✓	✓	~	✓
S10	**Phase segregation**	Slows some deformation mechanisms	✓	✓	~	✓
	Macroscopic geometric evolution:					
S11	**Folding**	Interrupt weak layers & rotate strong layers away from the shear plane	✓	✓	✓	✓

✓= yes, ~ = possibly, X = no

lead to porosity reduction and strengthening (Woodcock et al., 2007; Callahan et al., 2020). The hydrothermal phases may be precipitated in veins or as breccia cements (Fig. 2a,h,i), may infill existing porosity, or may replace existing minerals (Wintsch and Yeh, 2013). These new phases may be inherently stronger than the existing minerals (e.g., strong hydrothermal quartz versus weak clay minerals, Callahan et al., 2020); they may be stronger due to their coarse grain size (e.g., coarse-grained vein quartz in fine-grained ultramylonitic quartzite); or they may strengthen the rock by destroying mechanical anisotropies (e.g., "flooding" of a rock by massive hydrothermal quartz versus highly foliated schist), filling in porosity, or cementing poorly consolidated material (e.g., Wintsch and Yeh, 2013). Small amounts of hydrothermal minerals may be precipitated rapidly due to co-seismic pressure drops, or larger volumes may precipitate more slowly from advecting fluids during the interseismic period (Williams and Fagereng, 2022).

Various types of hydrothermal ore deposits illustrate the ability of hydrothermal fluids to precipitate significant quantities of material over time. For example, shear-hosted orogenic gold deposits typically comprise abundant gold-bearing quartz ± sulphide ± carbonate veins, precipitated in the BDT (Sibson et al., 1988; Goldfarb et al., 2005; Honsberger et al., 2020). To form these deposits, hydrothermal fluids derived from prograde metamorphic devolatilization at depth carry Si, S, CO_2, and Au in solution (Phillips and Powell, 2010; Groves et al., 2018); however, when seismic ruptures create open spaces (such as in releasing bends along faults; Groves et al., 2018), the resultant sudden drop in confining- and fluid pressure drastically lowers the solubility of quartz, sulphide and carbonate, which precipitate as veins (Goldfarb et al., 2005). Gold, which is held in solution as a sulphide complex (Phillips and Powell, 2010), also precipitates out as the S is removed from the fluid (Goldfarb et al., 2005). Orogenic gold deposits are typically built up over numerous such episodes, reflecting numerous seismic cycles. A similar process controls precipitation of vein-hosted epithermal deposits (Sanchez-Alfaro et al., 2016), and while these form in the shallow crust (Rhys et al., 2020), they nonetheless reflect processes of fluid flow and rupture-related precipitation that are active throughout the seismic portion of the crust. In such systems, significant quantities of vein-fill material can be precipitated over time, such that evidence of deformed fault rock may be completely obliterated (Rhys et al., 2020).

4.4 Other microstructural changes

Several other microstructural changes may also lead to shear zone strengthening:

(S7) Strain (or work) hardening occurs in grains deforming by dislocation glide, when dislocations build up and become tangled, increasing the stress required for dislocation motion and thus strengthening the grains (Passchier and Trouw, 2005; Wallis et al., 2018). Optical effects of strain hardening include undulatory extinction (due to lattice distortion) and deformation lamellae (Passchier and Trouw, 2005). Strain hardening may be counteracted by recovery and dynamic recrystallization, which are enhanced by elevated temperatures and the presence of water (Tullis and Yund, 1989; Palazzin et al., 2018; Pongrac et al., 2022). At the conditions of the BDT, which is at the low-temperature, high-stress end of the crystal plastic deformation range, such dislocation climb is suppressed (Ashby and Verall, 1978), limiting grain recovery and dynamic recrystallization, and resulting in strain hardening.

Ongoing shear can lead to the **(S8) rotation of anisotropies** (such as foliations or compositional banding) which then become unfavorably oriented for creep, leading to strengthening of the rock. This is counteracted by the development of new anisotropies in the correct orientation for creep. For example, progressive rotation of S and C surfaces can lead to their abandonment, and the formation of new, more suitably oriented C' surfaces (Handy et al., 2007).

Pressure solution, or more generally, **(S9) dissolution-precipitation**, refers to the dissolution of material in high-stress sites (such as grain-to-grain contacts), diffusive mass transfer in a fluid phase, and re-precipitation in lower-stress locations (forming, for example, pressure shadows) (Passchier and Trouw, 2005). This can contribute to fault strengthening by both cementation (by the newly precipitated material) and the increase of contact surface area between partially dissolved grains (Williams and Fagereng, 2022). However, it can also weaken faults by creating a tectonic fabric.

Finally, **(S10) phase segregation** can lead to strengthening: in quartz-mica-bearing rocks experiencing dissolution-precipitation creep, quartz is typically dissolved from high-stress sites and precipitated in lower-stress sites. This typically results in the formation of a differentiated fabric, with alternating quartz- and mica-rich bands, and may weaken the rock (e.g., W11, W13). However, pressure solution is faster along quartz:mica grain boundaries than along quartz:quartz boundaries, so increased differentiation of quartz and mica into separate bands will decrease the rate of pressure solution, as the number of quartz:mica interfaces decrease (Schmidt and Platt, 2022). This may cause a change in the dominant deformation mechanism (from diffusion creep to, e.g., dislocation creep, Schmidt and Platt, 2022), or it may conceivably lead to some amount of strengthening.

4.5 Macroscopic geometric evolution

(S11) Folding during shearing can significantly strengthen the bulk rheology of a shear zone, by interrupting the continuity of weak layers and rotating rigid layers away from the shear plane (Melosh et al., 2018). Active shear folds develop by buckling in rheologically layered material, where the layers themselves exert a mechanical influence on the folding process (Alsop and Holdsworth, 2012; Melosh et al., 2018). Such folds initiate at anisotropies or viscosity contrasts within the shear zone (Carreras et al., 2005), and may range in scale from millimeter- to decameter- wavelengths

(Fig. 2f,g; Melosh et al., 2018).

The strengthening effect of active shear folding can be counteracted over time by rotational weakening, as the fold limbs are progressively rotated into parallelism with the shear plane (Cobbold, 1977; Melosh et al., 2018). This occurs because, although the folds initially form by active buckling of rheologically distinct layers, they are subsequently flattened and smeared out by ongoing shear, leading to fold tightening and eventually transposition (rotational weakening, Cobbold, 1977; Carreras et al., 2005). In addition, Melosh et al. (2018) propose that shear folding focuses deformation in areas of high stress, promoting localized grain-size reduction by dynamic recrystallization and/or pseudotachylite formation, and thus re-weakening the shear zone.

5 Discussion: Likely mechanisms

Of the various weakening and strengthening mechanisms described above, several fulfill the criteria of 1) being reversible or able to be counteracted at constant PT conditions; 2) operating to change the fault strength from its current state, 3) potentially operating at the observed 20 – 25 m length scale or centennial-millennial timescale, and 4) being active within the BDT. These include fluid-driven weakening mechanisms counteracted by intra- and intergranular dehydration mechanisms; weakening by fabric development and microstructural evolution counteracted by the precipitation of hydrothermal cements and veins; strengthening by strain hardening counteracted by dynamic recrystallization and other microstructural recovery processes; and strengthening by folding counteracted by rotational weakening.

We now explore the workings of each of these paired mechanisms in more detail, and speculate on possible scenarios in which they may result in the variations in relative fault strength inferred from paleoseismic evidence (e.g., Weldon et al., 2004; Dolan et al., 2007, 2016, 2024; Zinke et al., 2017, 2019, 2021; Hatem et al., 2020).

5.1 Fluids (dehydration – rehydration cycles)

As outlined in Section 4, fluids play a major role in weakening shear zones. Intergranular fluids, present in fractures and microfractures, in pore spaces, and along grain boundaries, contribute to reaction weakening, diffusional deformation, enhanced grain boundary mobility, and the weakening effect of fluid-filled porosity, and their accumulation may result in fluid overpressure and hydraulic fracturing (e.g., Mancktelow and Pennacchioni, 2004; Okazaki et al., 2021). In contrast, intracrystalline fluids, present as OH- defects and/or fluid inclusions within mineral grains, enable hydrolytic weakening (Kronenberg and Tullis, 1984; Stünitz et al., 2017). All of these weakening mechanisms require fluids to be present within the shear zone, between mineral grains, and hydrolytic weakening further requires that water is present within the grains. Upon the removal of the inter- and intragranular fluids (which can be either lost from the shear zone or consumed by precipitation of new hydrous phases), these weakening mechanisms will cease, resulting in a relative strengthening of the shear zone. For this to result in periodic variations in shear zone strength, the BDT must experience net-hydration at some times, and net-dehydration at others, rather than a continuous flow-through of fluids. Finally, to drive the observed variations in fault slip rates, these hydration/dehydration cycles must occur over timescales commensurate with ~20 – 25 m slip.

What drives fluid flow through the crust? Throughout the crust, fluids will move along a hydraulic gradient (from a higher fluid pressure in hydrous regions, to a lower fluid pressure in dry rocks), provided there is permeability through which they can flow (Cox, 2005). Fluids produced at depth by magmatic or metamorphic devolatilization will therefore typically move upwards (Cox, 2005; Connolly, 2010), and meteoric waters may penetrate downwards into permeable shear zones (Kerrich, 1986; Whitehead et al., 2020), although permeability anisotropy and the complex patterns of tectonic pressure created during deformation may also result in significant along-strike flow (Cox, 2005). Thus, although fluid flow is driven by fluid pressure gradients, the direction of fluid flow will be strongly controlled by the distribution and orientation of permeability (Cox, 2005). Active shear zones, in which deformation and (at least transient) permeability are strongly localized, are thus major fluid channels (e.g., Kerrich, 1986; Cox, 2005).

The specific stress state of a shear zone will affect its internal fluid pressure, and thus the direction of fluid flow (into, out of, or along the shear zone; provided permeability exists). Depending on their orientation relative to the tectonic stress field, shear zones may be thinned during deformation ("positive stretching faults" of Means, 1989). These thinning shear zones will be overpressured relative to their host rocks, so fluids will be expelled (Mancktelow, 2002, 2006, 2008) unless trapped by impermeable layers (Menegon and Fagereng, 2021). Alternatively, shear zones oriented in the field of instantaneous shortening will be thickened, reducing the mean stress within the shear zone, and causing fluids to flow into the shear zone (Mancktelow, 2002, 2006, 2008), in much the same way that fluids will drain into an extensional fracture from the surrounding rock. Shear zones may therefore change from being over- to underpressured if they rotate from the field of instantaneous extension to that of instantaneous shortening (or if the regional stress field changes). This could cause fluids to initially flow out of a thinning, overpressured shear zone, but then flow into the shear zone as it becomes underpressured. However, it is difficult to envisage a realistic tectonic scenario that would result in these changes being cyclic, so the internal pressure of a shear zone – while important for governing fluid flow in or out of the shear zone – is unlikely to drive the observed ~20 – 25 m-scale strength variations.

Within shear zones, permeability and fluid flow are highest in regions experiencing local extension, such a releasing bends, fault jogs, and fold hinges (Sibson, 1987; Cox, 2005). Accordingly, most orogenic gold deposits are associated with fault jogs and bends, dilatant structures in competent rock units surrounded by

more ductile material, antiformal fold hinges, and the boundaries between more- and less- rigid lithologies (e.g., Groves et al., 2018).

How do fluids move through the brittle upper crust? In the brittle, seismogenic crust, the permeability that enables fluid flow may be long-lasting (faults and fractures that remain open for some time, or simply a permeable lithologic unit), or it may be transient (such as along co-seismic structures, or through hydraulic fractures driven by transient fluid overpressure). For example, Sibson (1987) postulated that during seismic ruptures, dilation within releasing bends or jogs causes an abrupt reduction in fluid pressure, resulting in boiling (and precipitation of hydrothermal mineral phases) as well as suddenly drawing fluid in from surrounding structures (the "suction pump model", Sibson, 1987; Sibson et al., 1988). As evidence, he cites the mineral textures observed in epithermal deposits, which are consistent with rapid precipitation during multiple episodes of boiling due to sudden pressure drops (e.g., Sanchez-Alfaro et al., 2016; Gülyüz et al., 2018; Rhys et al., 2020), and the concentration of these deposits in releasing bends and jogs along faults.

Fluids may also play a more active role in faulting, as suggested by the "fault valve model" (Sibson et al., 1988), based largely on observations of vein geometries in orogenic gold deposits. This model suggests that if a fault remains locked and relatively impermeable during the interseismic period (such as, for example, a high-angle reverse fault that is unfavorably oriented for reactivation in a compressive stress regime), fluids may accumulate in its deeper aseismic portions and build up to suprahydrostatic pressures. This drives the opening of some flat-lying veins adjacent to the main fault, but the fault itself remains sealed. Once the rising fluid pressure exceeds the lithostatic load, however, it triggers seismic failure of the fault, creating fracture permeability along the ruptured fault, draining of the overpressured fluid, and precipitation of veins along the fault. These veins help to hydrothermally seal the fault, leading to another interseismic period and repeating the cycle.

Such processes may thus drive major changes in fault permeability and fluid flow in the mid- to upper crust during the seismic cycle (Cox, 2005). However, they do not address how fluids move into or through the ductile BDT during the interseismic period; how the fluid content of the shear zone may vary over timescales longer than the seismic cycle; or how intragranular fluid may move in and out of mineral grains within the shear zone.

How do fluids move through ductile rocks? It is commonly assumed that brittle dilational deformation, driven by near-lithostatic fluid pressures (hydraulic fracturing), and manifest as veins, fractures, and grain-scale microcracks, is required to create pathways for fluid flow below the BDT (Connolly and Podladchikov, 2004; Cox, 2005; Mancktelow, 2006). Several experimental studies summarized by Cox et al. (2001) found that brittle, microcrack-dominated permeability persists well into the regime of dominantly ductile, crystal plastic deformation, if fluid pressures are sufficiently high.

However, recent studies have shown that fluid flow can also occur in rocks deforming by purely ductile processes. High-resolution microstructural studies on natural, ductile mid-crustal shear zones have found that aqueous fluids are concentrated in high strain areas, and occur in pores along grain boundaries (Fusseis et al., 2009; Menegon et al., 2015; Précigout et al., 2017). These studies propose that fluids move through the shear zones by creep cavitation, the closing and opening of successive cavities between imperfectly fitted grains, as the grains slide past one another during viscous grain boundary sliding. This process may create grain-scale fluid pressure differences, causing fluids to migrate through wholly ductile rocks under the effect of a "granular fluid pump" (Fusseis et al., 2009). Grain boundary porosity potentially linked to creep cavitation has also been identified in coarser-grained natural mylonites, in which the dominant deformation mechanism may have been dislocation creep (Mancktelow et al., 1998). Experimental work on fine-grained olivine deformed under ductile conditions highlights this tendency for water to move into actively recrystallizing zones, and the importance of grain boundary porosity created by creep cavitation for the storage of water in these high-strain zones (Précigout et al., 2019). Similarly, studies of natural ductile shear zones show that fluids may move through transient dilatant sites created at rheological contrasts (such as between brittle porphyroclasts and their ductile matrix; Kolb, 2008; Spruzeniece and Piazolo, 2015).

In addition, fluids may migrate through the ductile crust by grain boundary diffusion between grains, or volume diffusion or the migration of fluid inclusions through grains (e.g., Graham et al., 1998; Gleason and DeSisto, 2008; Putnis and Austrheim, 2010). Diffusion through grains, however, is slow (Fig. 3; Putnis and Austrheim, 2010) and its role in fluid transport is likely insignificant compared to that of deformation-enhanced permeability. Furthermore, where the rocks are metastable or the fluid is in disequilibrium, fluids may move through nominally impermeable rock by reactive fluid flow, enabled by a transient reaction-induced permeability increase (Beinlich et al., 2020). In the absence of shear zones, fluids generated at depth may move through the ductile mid- to lower crust by means of porosity waves, driven by the interplay between fluid production and rock compaction (Connolly, 1997, 2010). These theoretical constructs provide a potential mechanism for driving episodic, upwards movement of fluids, despite a continuous production of fluids at depth (Connolly, 1997; Cox, 2005).

In summary, fluid production and tectonic deformation create large-scale fluid pressure gradients, which drive the movement of fluids through the crust (Mancktelow, 2002, 2008; Cox, 2005). This fluid flux is largely concentrated into shear zones (Kerrich, 1986; Cox, 2005), where deformation and metasomatic reactions create transient permeability through processes that may be purely ductile (such as creep cavitation, Fusseis et al., 2009) or may involve transient embrittlement driven by high fluid pressures (Connolly and Podladchikov, 2004; Cox, 2005).

Timescales of fluid movement in/out of the BDT: The timescale over which porosity waves may operate will be linked to the rates of fluid production at depth (Connolly, 2010). Numerical modelling of a compacting crustal column undergoing fluid production by metamorphic devolatilization at depth, and cut by a vertical high-permeability shear zone, suggests that the interplay between the regions of different permeabilities, and between fluid transport through the shear zone versus by porosity waves, may lead to variations in the fluid flux up the shear zone over periods of ~50 kyr (Connolly, 2010).

Although the mechanism remains unclear, geological evidence exists for cases of fluid pulses moving through the crust (and specifically through shear zones) at kyr-timescales. Oxygen isotope gradients in various minerals provide evidence for fluid flow events, at amphibolite-facies conditions, that may have lasted as little as 10^3 – 10^4 years (van Haren et al., 1996; Graham et al., 1998). Thermal modelling of apatite (U-Th)/He around an active normal-sense fault in Nevada suggests that the fault has experienced 30 – 40 individual fluid pulses over the last ~250 ky, each lasting ~1 ky (Louis et al., 2019). These authors propose that the fluid flow is triggered by seismic events, and that the system then re-seals itself over ~1 ky by the formation of clays and silicates in the damage zone. However, existing paleoseismic data for the most recent earthquake (~7,500 years ago; Wesnousky et al., 2005) does not correspond to thermal model estimates for the most recent hydrothermal pulse (beginning ~3,000 years ago; Louis et al., 2019), suggesting an alternative mechanism may be driving the fluid pulses.

Similarly, Hickey et al. (2014) used apatite fission-track thermochronology and thermal modelling to estimate the duration of fluid flow responsible for forming an upper-crustal Carlin-style gold deposit, and obtained a maximum duration of <15 to 45 ka. U-Th dating of multiple generations of carbonate in the brittle Monte Morrone Fault System of Italy yields a range of Middle Pleistocene ages, with a 10 – 15 ky cyclicity (Vignaroli et al., 2022). Both Hickey et al. (2014) and Vignaroli et al. (2022) invoke coseismic permeability as leading to the observed hydrothermal pulses; however, these repeated pulses may also reflect independent fluid flux events that span multiple seismic cycles.

Moving water into/out of crystals: The above discussion describes possible mechanisms for introducing fluids into the intergranular/pore spaces in the BDT, over kyr timescales. These intergranular fluids may then drive weakening mechanisms such as enhancing diffusional deformation and hydrofracturing. To understand the possible weakening contributions of intragranular fluids, however, the potential mechanisms and timescales of moving fluids in- and out- of mineral grains must be investigated:

Water may enter minerals by diffusion (volume diffusion through the crystal lattice, pipe diffusion along dislocations, or diffusion along subgrain boundaries and twin lamellae); by movement with migrating dislocations or grain boundaries; or along cracks and microfractures (Graham et al., 1998; Gleason and DeSisto, 2008). Water can penetrate up to 100 µm into quartz in just 100,000 years by volume diffusion at typical BDT conditions (Gleason and DeSisto, 2008), or ~200 µm into calcite in ~10^3 – 10^4 years at amphibolite facies temperatures (Fig. 3; Graham et al., 1998). However, the equilibrium solubility of water in quartz is low (~10-200 H:10^6 Si), whereas water-weakened quartz is characterized by much higher abundances of water (~10^2 – 10^3 H:10^6 Si, Kronenberg, 1994). It is therefore unlikely that sufficient water can diffuse into the quartz crystal lattice to cause significant weakening (Kronenberg et al., 1986). In contrast, microcracking can significantly enhance the penetration of water into grains, and has the added benefit of delivering water in the form of fluid inclusions, which are currently thought to be the main culprit in hydrolytic weakening (Kronenberg et al., 1986; Stünitz et al., 2017; Palazzin et al., 2018). Abundant fluid inclusions along lines or planes within apparently whole grains are evidence for the infiltration of fluid into microcracks, which are subsequently healed (Fig. 2d; Gleason and DeSisto, 2008; Stünitz et al., 2017).

Evidence from both natural and experimental shear zones shows that dynamic recrystallization, associated with both dislocation- and diffusion-creep, tends to expel water and fluid inclusions from deforming mylonites and ultramylonites (Finch et al., 2016; Palazzin et al., 2018; Kronenberg et al., 2020; Singleton et al., 2020; Song et al., 2020), if the recrystallizing rocks were initially water-rich (Palazzin et al., 2018). In contrast, if the deforming rock was initially dry, the intracrystalline water content may increase during dynamic recrystallization (Palazzin et al., 2018). This highlights the importance of hydraulic gradients in determining the direction of fluid movement.

Microcracking is therefore the most efficient means of introducing intracrystalline water, in the form most conducive to weakening of the crystal (fluid inclusions), and it is most likely to affect dry, strong crystals (Stünitz et al., 2017). In contrast, the presence of intragranular water enhances rates of dynamic recrystallization, which then acts to expel this water (e.g., Palazzin et al., 2018; Kronenberg et al., 2020).

These observations may tie into the observed temporal variations in shear zone strength. During periods of fast fault slip, when minerals within the BDT are relatively hydrous and thus weak, higher strain rates and the availability of water will drive enhanced dynamic recrystallization (e.g., Palazzin et al., 2018) in the ductile mylonites and ultramylonites (Fig. 4). This results in a net loss of intracrystalline water from the recrystallizing grains (Palazzin et al., 2018; Kronenberg et al., 2020), reducing the effect of hydrolytic weakening and strengthening the grains, and thus the shear zone (e.g., Oliot et al., 2014; Finch et al., 2016). The locus of deformation shifts into weaker material (in this case, a mechanically complementary, but now relatively weaker, nearby shear zone). Here our model differs from that of Oliot et al. (2014) and Finch et al. (2016): they propose that the water expelled during dynamic recrystallization in their studied shear zones moved into the adjacent, drier wall rocks, causing weak-

ening and strain localization in the margins adjacent to the now-hardened, dehydrated shear zone core, leading to progressive widening of the cumulative ultramylonite zone. In contrast, we suggest that, in some cases, the expelled water moves upwards out of the BDT, enabling wholesale strengthening of the shear zone (e.g., Dolan and Meade, 2017), and causing deformation to become concentrated in an entirely different shear zone. This marks the start of a period of relatively slow slip, during which the relatively dry, strong grains deform by microcracking. This, in turn, enables the influx of water into the grain interiors (Stünitz et al., 2017; Palazzin et al., 2018), which once again weakens the grains and heralds the start of a fast, weak period. The duration of these slow and fast periods will depend on how long it takes to strengthen the shear zone through dynamic recrystallization-driven grain dehydration and/or weaken it by microcracking-driven rehydration, and on the strength threshold that must be reached for displacement to switch from one shear zone to another. Note that this scenario applies to non-reactive rocks that are in equilibrium with the fluid. We suggest that most shear zones are non-reactive, after their initial formation and potential weakening during early reactive fluid flow and hydration, because the resulting hydrous mineral assemblage will remain stable unless metamorphic conditions change (see Section 3.1).

Therefore, fluids may contribute to the observed variations in fault slip rates, with dynamic recrystallization during fast periods (enhanced by abundant fluid inclusions within the grains) driving grain dehydration and shear zone strengthening, and micro-cracking (enhanced because the grains are anhydrous and thus strong) and diffusion during slow periods allowing rehydration and weakening of the grains and thus the shear zone. Fluids may thus be responsible for the observed ~20 – 25 m-scale variations in fault slip rates, but only if they are taken up and expelled by shear zones over the correct length- and time-scale. Fluids may be supplied in pulses that last hundreds to thousands of years. Such pulses may be related to porosity waves (e.g., Connolly, 2010), or some other process that episodically supplies fluids from depth.

5.2 Hydrothermal cementation and fabric development/microstructural weakening

During the interseismic period, crystal plastic deformation in the BDT leads to progressive weakening of the rock by fabric development. Even once the rock has developed a tectonic fabric (foliation, cleavage, compositional banding), ongoing deformation drives microstructural weakening processes, such as the development of viscous anisotropy and interconnected weak layers, and grain size reduction by dynamic recrystallization (aided by cataclasis and pseudotachylite formation during co-seismic deep penetration of brittle fractures), further weakening the shear zone.

However, if hydrothermal fluids with sufficient dissolved solutes are present, these weakening processes may be counteracted by the strengthening effect of hydrothermal cementation (e.g., Woodcock et al., 2007). Strengthening by hydrothermal cementation requires fluid ingress and mineral precipitation. In epithermal and orogenic gold deposits, it has long been recognized that co-seismic dilation of faults or fractures leads to a rapid pressure drop, causing fluid boiling (flash vaporization), supersaturation of dissolved material, and rapid crystal nucleation and growth, with relatively slower mineral precipitation during the following interseismic period (Sibson, 1987; Sibson et al., 1988; Weatherley and Henley, 2013; Sanchez-Alfaro et al., 2016; Gülyüz et al., 2018; Rhys et al., 2020). However, recent work shows that only negligible amounts of hydrothermal cement (~0.02% of the dilational volume, for quartz and a 1.5 times difference between lithostatic and hydrostatic pressure) can be precipitated by co-seismic dilation and flash vaporization, due to the limited amount of fluid available in the closed system represented by the dilational volume (Williams and Fagereng, 2022). Precipitation is similarly negligible if fluid is allowed to flow in from along the fault, because fluid pressure in the dilatant site is rapidly recovered (Williams and Fagereng, 2022). These authors found that significantly more material may be precipitated by the advection of large volumes of fluids upwards through the shear zone over time, and Woodcock et al. (2007) show that significant volumes of carbonate cement may be precipitated during interseismic periods.

Hydrothermal cementation is thus unlikely to cause significant strengthening during a single seismic cycle (Williams and Fagereng, 2022). However, the cumulative build-up of hydrothermal veins and/or hydrothermally cemented material over a number of seismic cycles, and including the volumes precipitated during inter-seismic periods, can add up to a significant volume of material, which will have a significant effect on the shear zone strength. Studies using modern geothermal systems and numerical modelling show that earthquakes as small as $M_w < 2$ can trigger boiling and epithermal quartz-gold deposition, with numerous earthquakes required to build up an economic mineral deposit (Sanchez-Alfaro et al., 2016; Rhys et al., 2020). Such seismic events, each creating fractures or faults and driving the hydrothermal cementation that heals them, repeated over thousands of years, can deposit large volumes of quartz and carbonate along with the ore minerals (Sibson, 1987; Sibson et al., 1988; Goldfarb et al., 2005; Rhys et al., 2020), resulting in significant shear zone strengthening. For example, Gülyüz et al. (2018) describe mineralized quartz veins up to 13.6 m wide, with a strike length of 240 m. Veins in orogenic gold deposits typically vary from meters to tens of meters in width, and deposits comprising multiple veins may be wider than 1 km and extend 1 – 3 km vertically, and in notable cases extend 5 – 8 km along strike (Goldfarb et al., 2005). By applying $^{40}Ar/^{39}Ar$ dating to adularia in a Pleistocene low-sulfidation epithermal gold deposit, Sanematsu et al. (2006) showed that the mineralized quartz-adularia-smectite Hosen-1 vein, 1 – 3 m wide and 300 – 400 m in strike length, formed episodically by fracturing and subsequent vein infilling over ca.

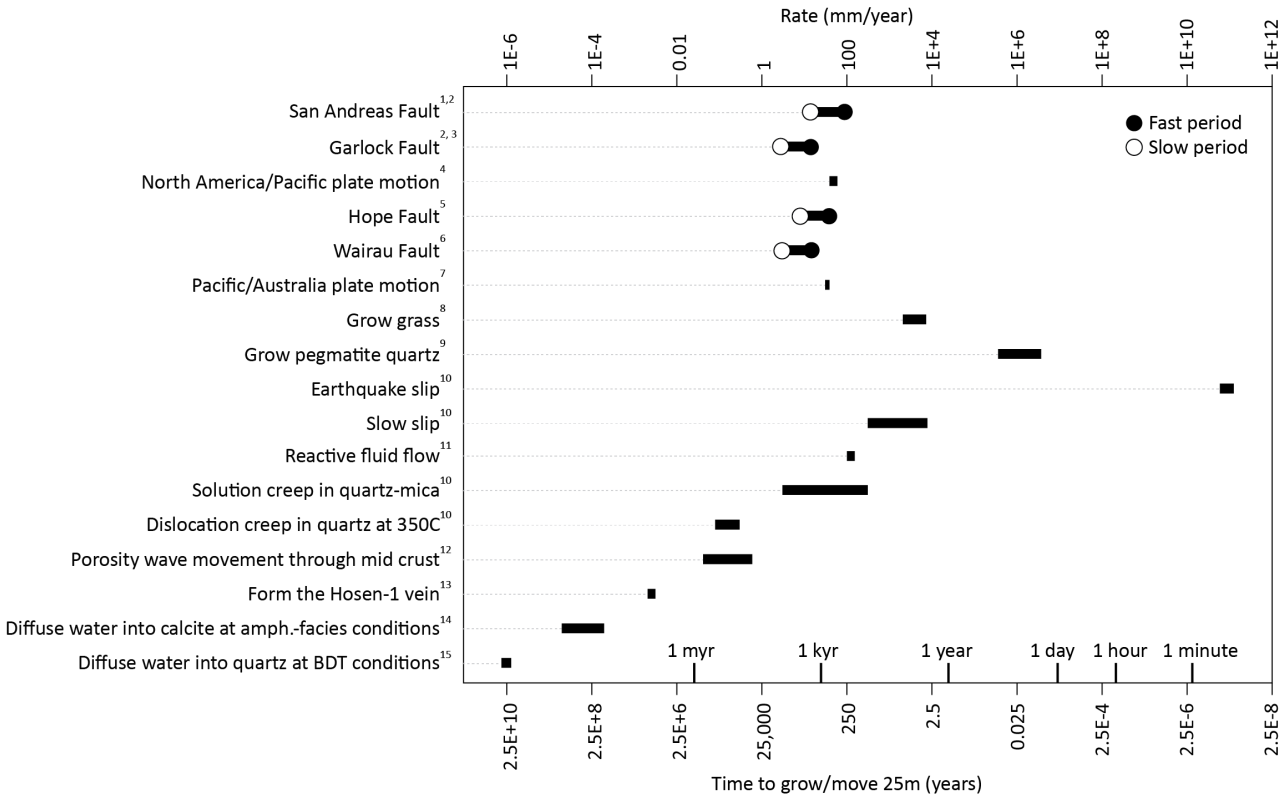

Figure 3 Timescales of fault slip compared to timescales of various geological processes. Adapted from Phelps et al. (2020), with data from 1) Weldon et al. (2004); 2) Dolan et al. (2016); 3) Dawson et al. (2003); 4) Gauriau and Dolan (2021); 5) Hatem et al. (2020); 6) Zinke et al. (2021); 7) Dolan et al. (2024); 8) Peacock (1976); 9) Phelps et al. (2020); 10) Rowe and Griffith (2015); 11) Beinlich et al. (2020); 12) Connolly (2010); 13) Sanematsu et al. (2006); 14) Graham et al. (1998); 15) Gleason and DeSisto (2008); and references therein.

260,000 years, with individual bands of the vein separated by 30,000 – 110,000 years. Mineral textures within each band are consistent with rapid precipitation due to boiling (Sanematsu et al., 2006).

Co-seismic rupturing in both the BDT and brittle upper crust thus creates permeability, weakening the shear zone, but also enables fluid ingress and hydrothermal cementation that destroys the permeability and strengthens the shear zone (Sibson, 1987; Gülyüz et al., 2018). This weakening/strengthening occurs during each earthquake cycle. However, the progressive buildup of hydrothermal mineralization over many earthquake cycles can create large volumes of massive, coarse-grained material that strengthens the shear zone over a longer timescale, possibly comparable to the 260,000-year timescale required to form the Hosen-1 epithermal vein (Sanematsu et al., 2006).

Strengthening due to hydrothermal cementation is likely to be most effective during periods of relatively fast fault slip, when abundant earthquakes drive regular fluid pressure fluctuations and thus hydrothermal mineral precipitation (Fig. 4). Although fabric development and microstructural evolution likely operate through both fast- and slow periods, their weakening effects may be swamped during the fast periods by the strengthening effects of hydrothermal cementation. Less-frequent earthquakes during the slow periods allow for longer interseismic periods, and thus more time for the predominantly ductile fabric-forming mechanisms to operate, which weaken the shear zone.

These paired weakening and strengthening mechanisms may therefore drive the inferred variations in shear zone strength. The estimated time required to form the Hosen-1 vein epithermal deposit (ca. 260,000 years, Sanematsu et al., 2006) provides an approximation of the time required to precipitate a significant volume of hydrothermal cement. This is notably longer than the hundreds- to thousands of years typically observed between fast/slow cycles on faults (Fig. 3; e.g., Weldon et al., 2004; Dolan et al., 2024), suggesting either that less hydrothermal cementation is needed to significantly strengthen a fault, or that hydrothermal cementation operates too slowly to account for the observed fault behavior. We note, however, that cementation is likely a function of slip rate, such that significant volumes of hydrothermal material may accumulate faster in fault systems with a faster slip rate.

5.3 Microstructural strain hardening and recovery

As suggested by Dolan et al. (2007), microstructural strain hardening during fast periods may result in shear zone strengthening and slowing, allowing strain-hardened grains to then undergo microstructural recov-

ery ("anneal"), again weakening the shear zone and triggering another fast period.

Initially weak, unstrained grains will deform easily by dislocation glide, especially in the high-stress, low-temperature conditions prevalent at the BDT (Ashby and Verall, 1978), and at some strain rate, the rate of dislocation creation will be balanced by the rate of dislocation loss (by dislocation climb and other recovery mechanisms, Passchier and Trouw, 2005). During the higher strain rates of a fast period, however, dislocation glide may not keep up with the rate at which new dislocations are formed, resulting in an increase in dislocation density and an accumulation of dislocation tangles in the crystal lattice, and thus strain hardening (Passchier and Trouw, 2005; Dolan et al., 2007; Wallis et al., 2018). When the shear zone is strengthened to the point at which the bulk of the deformation shifts to a mechanically complementary but weaker fault, the shear zone enters a slow period. This slower strain rate allows the rate of dislocation climb to outpace the rate of dislocation creation, resulting in recovery, and thus weakening (Dolan et al., 2007).

As noted for other mechanisms, the duration of these alternating fast and slow periods will depend on how long it takes to strengthen and weaken the shear zone by strain hardening and recovery respectively, and on the strength threshold required for the shear zone to be temporarily, partially abandoned.

5.4 Folding and rotational weakening

The paired mechanisms of strengthening the shear zone during shear folding (Melosh et al., 2018) and rotational weakening (Cobbold, 1977) may account for the inferred variations in shear zone strengths, because shear folding is likely to be enhanced when the shear zone is weak and slipping rapidly and acts to strengthen it, whereas rotational weakening is likely to be dominant when the fault is strong and slow, and acts to weaken it (thus fulfilling Criterion 2). The two processes counteract one another, fulfilling Criterion 1 (reversibility), and both are active within the BDT, fulfilling Criterion 4.

During periods of relatively fast fault slip, deep penetration of large earthquakes creates brittle faults, veins, and pseudotachylites in the mylonites and ultramylonites of the typically ductile BDT (Fig. 4). The resulting competency (viscosity) contrasts create flow perturbations, which grow into active shear folds by buckling (Carreras et al., 2005) and strengthen the shear zone (Melosh et al., 2018). For a shear zone that is 30 m wide at the BDT (such as the Pofadder Shear Zone, South Africa, Melosh et al., 2018), and that comprises interbanded layers of ultramylonite and mylonite with strain rates of $3x10^{-10}$ and $3x10^{-13}$ s^{-1} respectively (Melosh et al., 2018), ~1 – 2 m-scale buckle folds can form in ~15 to 455 years as stronger, more slowly deforming layers buckle adjacent to weaker layers with higher strain rates. For an overall slip rate of ~15 – 90 mm/year (like the San Andreas fault; Weldon et al., 2004; Salisbury et al., 2018), buckle folds will reach these amplitudes (~1 – 2 m) after ~0.2 – 41 m of slip (depending on their position within the shear zone), which is comparable to the ~20 – 25 m of slip recorded during fast periods on various faults (Dolan et al., 2024). Importantly, buckle folds like these can strengthen the bulk rheology by 27% when their axial planes are at a high angle to the shear zone boundaries (see Fig. 9 in Melosh et al., 2018).

Although rotational weakening is ongoing during these fast periods, its weakening effect is swamped by the strengthening effect of the numerous, continuously produced shear folds. In addition, the folds themselves create local stress concentrations, focusing deformation and leading to higher strain rates that result in brittle failure (creating pseudotachylites or cataclasites) or enhanced ductile deformation. Both result in grain size reduction and local weakening (Melosh et al., 2018), but also enhance viscosity contrasts that can then generate new folds. Indeed, new folds are observed to form on the limbs of older shear folds as the limbs are progressively rotated (Ghosh and Sengupta, 1984). Eventually, however, the shear zone reaches the critical strength at which it is no longer the favorable structure, and most of the imposed displacement is transferred to another, mechanically complementary but currently weaker fault. This heralds the onset of a relatively slow slip period, characterized by slower ductile deformation, long interseismic periods, and few deep-penetrating ruptures. This results in a slower production rate of shear folds, allowing the effect of rotational weakening to become dominant, whereby ongoing simple shear rotates the fold axial planes into parallelism with the shear plane, removing their strengthening effect (Cobbold, 1977; Carreras et al., 2005; Melosh et al., 2018). Based on the relationship between shear strain and displacement (tangent of the shear strain equals displacement divided by distance across the shear zone), for folds near the center of a 30 m wide shear zone, ~175 m of slip is needed to rotate the axial plane by 85° (i.e., to rotate the fold into near parallelism with the shear plane). For folds near the shear zone edge, only ~11.5 m of slip is required.

6 Conclusions: Generalized model

The scenarios discussed above can be incorporated into a speculative generalized model to explain periodic strengthening and weakening of shear zones, summarized in Figure 4. It is important to note, however, that faults are complex natural systems with significant heterogeneity between and within individual examples, and that numerous possible feedbacks exist between the weakening and strengthening mechanisms we describe. It is therefore likely that a combination of mechanisms is active in any one shear zone at any one time, and that the specific combination of mechanisms at play will vary with tectonic setting, lithology, and time. Also note that we describe an inherently cyclic process, with conditions during periods of slow slip automatically preparing the shear zone for fast slip, and vice versa.

As a fault enters a slow period, it is initially relatively strong, dry, and slow. Strain rates in the underlying ductile shear zone are lower, slip rates on the overlying brit-

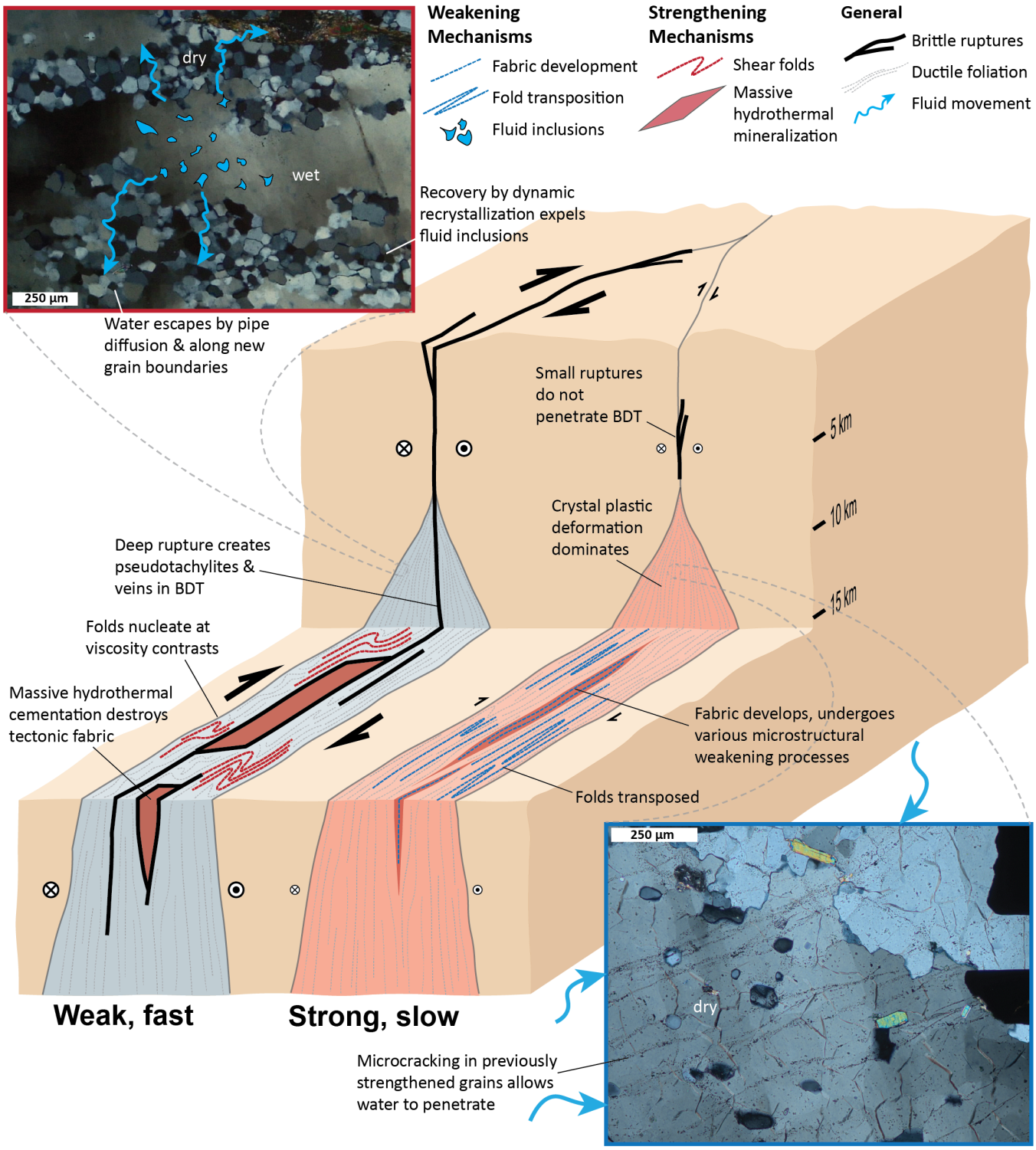

Figure 4 Schematic summary of strengthening and weakening mechanisms potentially responsible for variations in shear zone strength, inferred from alternating periods of fast- and slow-slip on mechanically complementary faults. A pair of mechanically complementary faults are illustrated. The left fault is weaker and thus in a "fast period", taking up most of the plate boundary motion, but experiences several processes that gradually strengthen it (shown in red). The right fault is stronger and thus in a "slow period", accommodating a smaller fraction of the displacement, but becomes gradually weaker over time due to the combined action of several weakening processes (shown in blue). Not to scale: note that the downward widening of the shear zone at the BDT is exaggerated for clarity.

tle fault are slower, and large earthquakes are rare. Mineral grains are initially dry and strong, making them more susceptible to microcracking and enhancing the penetration of water. Water is also able to diffuse into grains, without being continuously expelled by dynamic recrystallization (e.g., Kronenberg et al., 2020). This results in hydrolytic weakening and enhances easy glide (Griggs and Blacic, 1965).

During this time, ductile deformation predominates in the BDT, allowing the development of new tectonic

fabrics, viscous anisotropy, interconnected weak layers, and areas of phase mixing (Passchier and Trouw, 2005), all of which have a weakening effect. The lack of abundant new veins and pseudotachylites means fewer shear folds form, and existing folds are progressively smeared out by rotational weakening, resulting in an increasingly planar, weakened fabric (Cobbold, 1977). In mylonites and ultramylonites, the lower strain rate enables static recrystallization and recovery, and allows easy glide and thus the sweeping out of dislocation tangles (Passchier and Trouw, 2005; Dolan et al., 2007).

Slow ductile slip and few deep seismic ruptures therefore enable several weakening mechanisms, including fabric development and microstructural evolution, rotational weakening, easy dislocation glide without strain hardening, and hydrolytic weakening. This progressively weakens the shear zone, such that when its mechanically complementary partner is inevitably strengthened, our shear zone can again take up the majority of the imposed displacement and enter another fast period.

This period of relatively fast slip sees the fault experience a number of large earthquakes, resulting in deep rupture penetration and embrittlement of the BDT (e.g., Ellis and Stöckhert, 2004). These deep brittle failures each result in the precipitation of hydrothermal veins and cements, driven by the co-seismic pressure drops and the enhanced shear zone permeability that allows large-scale fluid advection (e.g., Williams and Fagereng, 2022). Over multiple earthquake cycles, significant volumes of massive hydrothermal material accumulate (e.g., Sanematsu et al., 2006). This strengthens the fault by cementing porosity and fractures, and by destroying tectonic fabrics and microstructures. In addition, the fractures, veins, and pseudotachylites formed in the BDT during large ruptures create major viscosity contrasts with the existing, interseismic mylonites and ultramylonites. These rheological contrasts provide nucleation points for the formation of shear folds, which also contribute to shear zone strengthening (Melosh et al., 2018). Furthermore, elevated strain rates in viscously deforming rock drive dislocation creep and dynamic recrystallization in the previously weakened, hydrous mineral grains. This dynamic recrystallization expels intracrystalline water (Palazzin et al., 2018; Kronenberg et al., 2020), removing the effect of hydrolytic weakening and thus strengthening the grains. This dehydration and strengthening also suppresses dislocation climb (Tullis and Yund, 1989; Palazzin et al., 2018; Pongrac et al., 2022), enhancing the development of dislocation tangles and resulting in strain hardening (Passchier and Trouw, 2005).

Fast ductile strain rates and numerous large earthquakes therefore enhance the occurrence of several strengthening mechanisms, including hydrothermal cementation, the destruction of tectonic fabrics and microstructures, the development of shear folds, strain hardening, and intragranular dehydration. After 10^2 – 10^3 years / 20 – 25 m of slip, the shear zone becomes strengthened to the point where it is no longer the most favorable structure for failure, and most of the imposed plate displacement shifts over to a different, mechanically complementary but currently weaker shear zone, starting the cycle anew.

Acknowledgements

We are grateful to Luca Menegon, Ian Honsberger, and an anonymous reviewer for valuable suggestions that greatly improved the manuscript, and to Åke Fagereng for his helpful comments and efficient editorial handling. This is NRCan contribution number 20230400.

7 Data and code availability

All potential weakening- and strengthening mechanisms are described in Supplementary Tables S1 and S2 respectively.

8 Competing interests

The authors have no competing interests.

References

Alsop, G. and Holdsworth, R. The three dimensional shape and localisation of deformation within multilayer sheath folds. *Journal of Structural Geology*, 44:110–128, Nov. 2012. doi: 10.1016/j.jsg.2012.08.015.

Ashby, M. and Verall, R. Micromechanisms of flow and fracture, and their relevance to the rheology of the upper mantle: Philosophical Transactions of the Royal Society of London. *Creep of Engineering Materials and of the Earth (Feb)*, 288(1350):59–93, 1978.

Behr, W. M. and Platt, J. P. Brittle faults are weak, yet the ductile middle crust is strong: Implications for lithospheric mechanics. *Geophysical Research Letters*, 41(22):8067–8075, Nov. 2014. doi: 10.1002/2014gl061349.

Beinlich, A., John, T., Vrijmoed, J. C., Tominaga, M., Magna, T., and Podladchikov, Y. Y. Instantaneous rock transformations in the deep crust driven by reactive fluid flow. *Nature Geoscience*, 13 (4):307–311, Mar. 2020. doi: 10.1038/s41561-020-0554-9.

Berryman, K. R., Cochran, U. A., Clark, K. J., Biasi, G. P., Langridge, R. M., and Villamor, P. Major Earthquakes Occur Regularly on an Isolated Plate Boundary Fault. *Science*, 336(6089):1690–1693, June 2012. doi: 10.1126/science.1218959.

Brace, W. F. and Kohlstedt, D. L. Limits on lithospheric stress imposed by laboratory experiments. *Journal of Geophysical Research: Solid Earth*, 85(B11):6248–6252, Nov. 1980. doi: 10.1029/jb085ib11p06248.

Bürgmann, R. and Dresen, G. Rheology of the Lower Crust and Upper Mantle: Evidence from Rock Mechanics, Geodesy, and Field Observations. *Annual Review of Earth and Planetary Sciences*, 36(1):531–567, May 2008. doi: 10.1146/annurev.earth.36.031207.124326.

Callahan, O. A., Eichhubl, P., and Davatzes, N. C. Mineral precipitation as a mechanism of fault core growth. *Journal of Structural Geology*, 140:104156, Nov. 2020. doi: 10.1016/j.jsg.2020.104156.

Campbell, L. R. and Menegon, L. Transient High Strain Rate During Localized Viscous Creep in the Dry Lower Continental Crust (Lofoten, Norway). *Journal of Geophysical Research: Solid Earth*, 124(10):10240–10260, Oct. 2019. doi: 10.1029/2019jb018052.

Cao, S., Neubauer, F., Liu, J., Bernroider, M., Cheng, X., Li, J., Yu, Z., and Genser, J. Rheological weakening of high-grade mylonites during low-temperature retrogression: The exhumed continental Ailao Shan-Red River fault zone, SE Asia. *Journal of Asian Earth Sciences*, 139:40–60, May 2017. doi: 10.1016/j.jseaes.2016.10.002.

Carreras, J., Druguet, E., and Griera, A. Shear zone-related folds. *Journal of Structural Geology*, 27(7):1229–1251, July 2005. doi: 10.1016/j.jsg.2004.08.004.

Cawood, T. and Platt, J. What controls the width of ductile shear zones? *Tectonophysics*, 816:229033, Oct. 2021. doi: 10.1016/j.tecto.2021.229033.

Ceccato, A., Menegon, L., and Hansen, L. N. Strength of Dry and Wet Quartz in the Low-Temperature Plasticity Regime: Insights From Nanoindentation. *Geophysical Research Letters*, 49(2), Jan. 2022. doi: 10.1029/2021gl094633.

Cobbold, P. R. Description and origin of banded deformation structures. II. Rheology and the growth of banded perturbations. *Canadian Journal of Earth Sciences*, 14(11):2510–2523, Nov. 1977. doi: 10.1139/e77-217.

Cole, J., Hacker, B., Ratschbacher, L., Dolan, J., Seward, G., Frost, E., and Frank, W. Localized ductile shear below the seismogenic zone: Structural analysis of an exhumed strike-slip fault, Austrian Alps. *Journal of Geophysical Research: Solid Earth*, 112 (B12), Dec. 2007. doi: 10.1029/2007jb004975.

Connolly, J. A. D. Devolatilization-generated fluid pressure and deformation-propagated fluid flow during prograde regional metamorphism. *Journal of Geophysical Research: Solid Earth*, 102(B8):18149–18173, Aug. 1997. doi: 10.1029/97jb00731.

Connolly, J. A. D. The Mechanics of Metamorphic Fluid Expulsion. *Elements*, 6(3):165–172, June 2010. doi: 10.2113/gselements.6.3.165.

Connolly, J. A. D. and Podladchikov, Y. Y. Fluid flow in compressive tectonic settings: Implications for midcrustal seismic reflectors and downward fluid migration. *Journal of Geophysical Research: Solid Earth*, 109(B4), Apr. 2004. doi: 10.1029/2003jb002822.

Cox, S. F. *Coupling between Deformation, Fluid Pressures, and Fluid Flow in Ore-Producing Hydrothermal Systems at Depth in the Crust*. Society of Economic Geologists, 2005. doi: 10.5382/av100.04.

Cox, S. F., Knackstedt, M. A., and Braun, J. Principles of Structural Control on Permeability and Fluid Flow in Hydrothermal Systems. In *Structural Controls on Ore Genesis*. Society of Economic Geologists, 2001. doi: 10.5382/Rev.14.01.

Dawson, T. E., McGill, S. F., and Rockwell, T. K. Irregular recurrence of paleoearthquakes along the central Garlock fault near El Paso Peaks, California. *Journal of Geophysical Research: Solid Earth*, 108(B7), July 2003. doi: 10.1029/2001jb001744.

Dolan, J., Van Dissen, R., Rhodes, E., Zinke, R., Hatem, A., McGuire, C., Langridge, R., and Grenader, J. One tune, many tempos: Faults trade off slip in time and space to accommodate relative plate motions. *Earth and Planetary Science Letters*, 625:118484, Jan. 2024. doi: 10.1016/j.epsl.2023.118484.

Dolan, J. F. and Meade, B. J. A Comparison of Geodetic and Geologic Rates Prior to Large Strike-Slip Earthquakes: A Diversity of Earthquake-Cycle Behaviors? *Geochemistry, Geophysics, Geosystems*, 18(12):4426–4436, Dec. 2017. doi: 10.1002/2017gc007014.

Dolan, J. F., Bowman, D. D., and Sammis, C. G. Long-range and long-term fault interactions in Southern California. *Geology*, 35 (9):855, 2007. doi: 10.1130/g23789a.1.

Dolan, J. F., McAuliffe, L. J., Rhodes, E. J., McGill, S. F., and Zinke, R. Extreme multi-millennial slip rate variations on the Garlock fault, California: Strain super-cycles, potentially time-variable fault strength, and implications for system-level earthquake occurrence. *Earth and Planetary Science Letters*, 446:123–136, July 2016. doi: 10.1016/j.epsl.2016.04.011.

Ellis, S. and Stöckhert, B. Elevated stresses and creep rates beneath the brittle-ductile transition caused by seismic faulting in the upper crust. *Journal of Geophysical Research: Solid Earth*, 109(B5), May 2004. doi: 10.1029/2003jb002744.

Finch, M. A., Weinberg, R. F., and Hunter, N. J. Water loss and the origin of thick ultramylonites. *Geology*, 44(8):599–602, June 2016. doi: 10.1130/g37972.1.

Fougere, D., Dolan, J., Rhodes, E., and McGill, S. Refined Holocene slip rate for the Western and Central segments of the Garlock Fault: Record of alternating millennial-scale periods of fast and slow fault slip. *Seismica*, 3(2), 2024. doi: 10.26443/seismica.v3i2.1202.

Frost, E., Dolan, J., Ratschbacher, L., Hacker, B., and Seward, G. Direct observation of fault zone structure at the brittle-ductile transition along the Salzach-Ennstal-Mariazell-Puchberg fault system, Austrian Alps. *Journal of Geophysical Research*, 116(B2), Feb. 2011. doi: 10.1029/2010jb007719.

Fusseis, F., Regenauer-Lieb, K., Liu, J., Hough, R. M., and De Carlo, F. Creep cavitation can establish a dynamic granular fluid pump in ductile shear zones. *Nature*, 459(7249):974–977, June 2009. doi: 10.1038/nature08051.

Gauriau, J. and Dolan, J. Comparison of geodetic slip-deficit and geologic fault slip rates reveals that variability of elastic strain accumulation and release rates on strike-slip faults is controlled by the relative structural complexity of plate-boundary fault systems. *Seismica*, 3(1), Feb. 2024. doi: 10.26443/seismica.v3i1.1119.

Gauriau, J. and Dolan, J. F. Relative Structural Complexity of Plate-Boundary Fault Systems Controls Incremental Slip-Rate Behavior of Major Strike-Slip Faults. *Geochemistry, Geophysics, Geosystems*, 22(11), Nov. 2021. doi: 10.1029/2021gc009938.

Ghosh, S. and Sengupta, S. Successive development of plane noncylindrical folds in progressive deformation. *Journal of Structural Geology*, 6(6):703–709, Jan. 1984. doi: 10.1016/0191-8141(84)90009-9.

Gleason, G. C. and DeSisto, S. A natural example of crystal-plastic deformation enhancing the incorporation of water into quartz. *Tectonophysics*, 446(1–4):16–30, Jan. 2008. doi: 10.1016/j.tecto.2007.09.006.

Goldfarb, R. J., Baker, T., Dubé, B., Groves, D. I., Hart, C. J., and Gosselin, P. *Distribution, character, and genesis of gold deposits in metamorphic terranes*. Society of Economic Geologists, 2005. doi: 10.5382/av100.14.

Graham, C. M., Valley, J. W., Eiler, J. M., and Wada, H. Timescales and mechanisms of fluid infiltration in a marble: an ion microprobe study. *Contributions to Mineralogy and Petrology*, 132(4): 371–389, Sept. 1998. doi: 10.1007/s004100050430.

Grall, C., Henry, P., Thomas, Y., Westbrook, G. K., Çağatay, M. N., Marsset, B., Saritas, H., Çifçi, G., and Géli, L. Slip rate estimation along the western segment of the Main Marmara Fault over the last 405–490 ka by correlating mass transport deposits. *Tectonics*, 32(6):1587–1601, Dec. 2013. doi: 10.1002/2012tc003255.

Grant Ludwig, L., Akciz, S. O., Arrowsmith, J. R., and Salisbury, J. B. Reproducibility of San Andreas Fault Slip Rate Measurements at Wallace Creek in the Carrizo Plain, CA. *Earth and Space Science*, 6(1):156–165, Jan. 2019. doi: 10.1029/2017ea000360.

Griffin, J. D., Stirling, M. W., Wilcken, K. M., and Barrell, D. J. A. Late Quaternary Slip Rates for the Hyde and Dunstan Faults, Southern New Zealand: Implications for Strain Migration in a

Slowly Deforming Continental Plate Margin. *Tectonics*, 41(9), Sept. 2022. doi: 10.1029/2022tc007250.

Griggs, D. T. and Blacic, J. D. Quartz: Anomalous Weakness of Synthetic Crystals. *Science*, 147(3655):292–295, Jan. 1965. doi: 10.1126/science.147.3655.292.

Groves, D. I., Santosh, M., Goldfarb, R. J., and Zhang, L. Structural geometry of orogenic gold deposits: Implications for exploration of world-class and giant deposits. *Geoscience Frontiers*, 9(4):1163–1177, July 2018. doi: 10.1016/j.gsf.2018.01.006.

Gülyüz, N., Shipton, Z. K., Kuşcu, I., Lord, R. A., Kaymakcı, N., Gülyüz, E., and Gladwell, D. R. Repeated reactivation of clogged permeable pathways in epithermal gold deposits: Kestanelik epithermal vein system, NW Turkey. *Journal of the Geological Society*, 175(3):509–524, Jan. 2018. doi: 10.1144/jgs2017-039.

Handy, M. R. Flow laws for rocks containing two non-linear viscous phases: A phenomenological approach. *Journal of Structural Geology*, 16(3):287–301, Mar. 1994. doi: 10.1016/0191-8141(94)90035-3.

Handy, M. R., Hirth, G., and Bürgmann, R. *Continental Fault Structure and Rheology from the Frictional-to-Viscous Transition Downward*, page 139–182. The MIT Press, May 2007. doi: 10.7551/mitpress/6703.003.0008.

Hansen, L. N., Zimmerman, M. E., and Kohlstedt, D. L. Laboratory measurements of the viscous anisotropy of olivine aggregates. *Nature*, 492(7429):415–418, Dec. 2012. doi: 10.1038/nature11671.

Hatem, A. E., Cooke, M. L., and Toeneboehn, K. Strain localization and evolving kinematic efficiency of initiating strike-slip faults within wet kaolin experiments. *Journal of Structural Geology*, 101:96–108, Aug. 2017. doi: 10.1016/j.jsg.2017.06.011.

Hatem, A. E., Dolan, J. F., Zinke, R. W., Langridge, R. M., McGuire, C. P., Rhodes, E. J., Brown, N., and Van Dissen, R. J. Holocene to latest Pleistocene incremental slip rates from the east-central Hope fault (Conway segment) at Hossack Station, Marlborough fault system, South Island, New Zealand: Towards a dated path of earthquake slip along a plate boundary fault. *Geosphere*, 16 (6):1558–1584, Oct. 2020. doi: 10.1130/ges02263.1.

Hawemann, F., Mancktelow, N. S., Wex, S., Camacho, A., and Pennacchioni, G. Pseudotachylyte as field evidence for lower-crustal earthquakes during the intracontinental Petermann Orogeny (Musgrave Block, Central Australia). *Solid Earth*, 9(3): 629–648, May 2018. doi: 10.5194/se-9-629-2018.

Hawemann, F., Mancktelow, N. S., Pennacchioni, G., Wex, S., and Camacho, A. Weak and Slow, Strong and Fast: How Shear Zones Evolve in a Dry Continental Crust (Musgrave Ranges, Central Australia). *Journal of Geophysical Research: Solid Earth*, 124(1): 219–240, Jan. 2019. doi: 10.1029/2018jb016559.

Hearn, E. and Bürgmann, R. The Effect of Elastic Layering on Inversions of GPS Data for Coseismic Slip and Resulting Stress Changes: Strike-Slip Earthquakes. *Bulletin of the Seismological Society of America*, 95(5):1637–1653, Oct. 2005. doi: 10.1785/0120040158.

Hickey, K. A., Barker, S. L. L., Dipple, G. M., Arehart, G. B., and Donelick, R. A. The Brevity of Hydrothermal Fluid Flow Revealed by Thermal Halos around Giant Gold Deposits: Implications for Carlin-Type Gold Systems. *Economic Geology*, 109(5): 1461–1487, May 2014. doi: 10.2113/econgeo.109.5.1461.

Hirth, G. and Tullis, J. Dislocation creep regimes in quartz aggregates. *Journal of Structural Geology*, 14(2):145–159, Feb. 1992. doi: 10.1016/0191-8141(92)90053-y.

Honsberger, I. W., Bleeker, W., Sandeman, H. A. I., Evans, D. T. W., and Kamo, S. L. *Vein-hosted gold mineralization in the Wilding Lake area, central Newfoundland: structural geology and vein evolution*. 2020. doi: 10.4095/326020.

Imber, J., Holdsworth, R. E., Butler, C. A., and Strachan, R. A. A reappraisal of the Sibson-Scholz fault zone model: The nature of the frictional to viscous ("brittle-ductile") transition along a long-lived, crustal-scale fault, Outer Hebrides, Scotland. *Tectonics*, 20(5):601–624, Oct. 2001. doi: 10.1029/2000tc001250.

Jordan, P. The rheology of polymineralic rocks — an approach. *Geologische Rundschau*, 77(1):285–294, Feb. 1988. doi: 10.1007/bf01848690.

Kerrich, R. Fluid transport in lineaments. *Philosophical Transactions of the Royal Society of London. Series A, Mathematical and Physical Sciences*, 317(1539):219–251, Apr. 1986. doi: 10.1098/rsta.1986.0033.

King, G. C. P. and Wesnousky, S. G. Scaling of Fault Parameters for Continental Strike-Slip Earthquakes. *Bulletin of the Seismological Society of America*, 97(6):1833–1840, Dec. 2007. doi: 10.1785/0120070048.

Kirkpatrick, J. D. and Rowe, C. D. Disappearing ink: How pseudotachylytes are lost from the rock record. *Journal of Structural Geology*, 52:183–198, July 2013. doi: 10.1016/j.jsg.2013.03.003.

Kolb, J. The role of fluids in partitioning brittle deformation and ductile creep in auriferous shear zones between 500 and 700 °C. *Tectonophysics*, 446(1–4):1–15, Jan. 2008. doi: 10.1016/j.tecto.2007.10.001.

Kozacı, O., Dolan, J. F., and Finkel, R. C. A late Holocene slip rate for the central North Anatolian fault, at Tahtaköprü, Turkey, from cosmogenic 10Be geochronology: Implications for fault loading and strain release rates. *Journal of Geophysical Research: Solid Earth*, 114(B1), Jan. 2009. doi: 10.1029/2008jb005760.

Kozacı, O., Dolan, J. F., Yönlü, O., and Hartleb, R. D. Paleoseismologic evidence for the relatively regular recurrence of infrequent, large-magnitude earthquakes on the eastern North Anatolian fault at Yaylabeli, Turkey. *Lithosphere*, 3(1):37–54, Feb. 2011. doi: 10.1130/l118.1.

Kronenberg, A. K. *Hydrogen speciation and chemical weakening of quartz*, page 123–176. De Gruyter, Dec. 1994. doi: 10.1515/9781501509698-009.

Kronenberg, A. K. and Tullis, J. Flow strengths of quartz aggregates: Grain size and pressure effects due to hydrolytic weakening. *Journal of Geophysical Research: Solid Earth*, 89(B6): 4281–4297, June 1984. doi: 10.1029/jb089ib06p04281.

Kronenberg, A. K. and Wolf, G. H. Fourier transform infrared spectroscopy determinations of intragranular water content in quartz-bearing rocks: implications for hydrolytic weakening in the laboratory and within the earth. *Tectonophysics*, 172(3–4): 255–271, Feb. 1990. doi: 10.1016/0040-1951(90)90034-6.

Kronenberg, A. K., Kirby, S. H., Aines, R. D., and Rossman, G. R. Solubility and diffusional uptake of hydrogen in quartz at high water pressures: Implications for hydrolytic weakening. *Journal of Geophysical Research: Solid Earth*, 91(B12):12723–12741, Nov. 1986. doi: 10.1029/jb091ib12p12723.

Kronenberg, A. K., Ashley, K. T., Francsis, M. K., Holyoke III, C. W., Jezek, L., Kronenberg, J. A., Law, R. D., and Thomas, J. B. Water loss during dynamic recrystallization of Moine thrust quartzites, northwest Scotland. *Geology*, 48(6):557–561, Mar. 2020. doi: 10.1130/g47041.1.

Kurt, H., Sorlien, C. C., Seeber, L., Steckler, M. S., Shillington, D. J., Cifci, G., Cormier, M., Dessa, J., Atgin, O., Dondurur, D., Demirbag, E., Okay, S., Imren, C., Gurcay, S., and Carton, H. Steady late quaternary slip rate on the Cinarcik section of the North Anatolian fault near Istanbul, Turkey. *Geophysical Research Letters*, 40(17):4555–4559, Sept. 2013. doi: 10.1002/grl.50882.

Leloup, P. H., Ricard, Y., Battaglia, J., and Lacassin, R. Shear heating in continental strike-slip shear zones: Model and field examples.

Geophysical Journal International, 136(1):19–40, Jan. 1999. doi: 10.1046/j.1365-246x.1999.00683.x.

Louis, S., Luijendijk, E., Dunkl, I., and Person, M. Episodic fluid flow in an active fault. *Geology*, 47(10):938–942, Aug. 2019. doi: 10.1130/g46254.1.

Maggi, M., Rossetti, F., Ranalli, G., and Theye, T. Feedback between fluid infiltration and rheology along a regional ductile-to-brittle shear zone: The East Tenda Shear Zone (Alpine Corsica). *Tectonics*, 33(3):253–280, Mar. 2014. doi: 10.1002/2013tc003370.

Mako, C. A. and Caddick, M. J. Quantifying magnitudes of shear heating in metamorphic systems. *Tectonophysics*, 744:499–517, Oct. 2018. doi: 10.1016/j.tecto.2018.07.003.

Mancktelow, N. S. Finite-element modelling of shear zone development in viscoelastic materials and its implications for localisation of partial melting. *Journal of Structural Geology*, 24(6–7): 1045–1053, June 2002. doi: 10.1016/s0191-8141(01)00090-6.

Mancktelow, N. S. How ductile are ductile shear zones? *Geology*, 34(5):345, 2006. doi: 10.1130/g22260.1.

Mancktelow, N. S. Tectonic pressure: Theoretical concepts and modelled examples. *Lithos*, 103(1–2):149–177, June 2008. doi: 10.1016/j.lithos.2007.09.013.

Mancktelow, N. S. and Pennacchioni, G. The influence of grain boundary fluids on the microstructure of quartz-feldspar mylonites. *Journal of Structural Geology*, 26(1):47–69, Jan. 2004. doi: 10.1016/s0191-8141(03)00081-6.

Mancktelow, N. S., Grujic, D., and Johnson, E. L. An SEM study of porosity and grain boundary microstructure in quartz mylonites, Simplon Fault Zone, Central Alps. *Contributions to Mineralogy and Petrology*, 131(1):71–85, Mar. 1998. doi: 10.1007/s004100050379.

Means, W. D. Stretching faults. *Geology*, 17(10):893, 1989. doi: 10.1130/0091-7613(1989)017<0893:sf>2.3.co;2.

Melosh, B. L., Rowe, C. D., Gerbi, C., Smit, L., and Macey, P. Seismic cycle feedbacks in a mid-crustal shear zone. *Journal of Structural Geology*, 112:95–111, July 2018. doi: 10.1016/j.jsg.2018.04.004.

Menegon, L. and Fagereng, A. Tectonic pressure gradients during viscous creep drive fluid flow and brittle failure at the base of the seismogenic zone. *Geology*, 49(10):1255–1259, July 2021. doi: 10.1130/g49012.1.

Menegon, L., Fusseis, F., Stünitz, H., and Xiao, X. Creep cavitation bands control porosity and fluid flow in lower crustal shear zones. *Geology*, 43(3):227–230, Mar. 2015. doi: 10.1130/g36307.1.

Montési, L. G. Fabric development as the key for forming ductile shear zones and enabling plate tectonics. *Journal of Structural Geology*, 50:254–266, May 2013. doi: 10.1016/j.jsg.2012.12.011.

Mulyukova, E. and Bercovici, D. The Generation of Plate Tectonics From Grains to Global Scales: A Brief Review. *Tectonics*, 38(12): 4058–4076, Dec. 2019. doi: 10.1029/2018tc005447.

Muto, J., Hirth, G., Heilbronner, R., and Tullis, J. Plastic anisotropy and fabric evolution in sheared and recrystallized quartz single crystals. *Journal of Geophysical Research*, 116(B2), Feb. 2011. doi: 10.1029/2010jb007891.

Okazaki, K., Burdette, E., and Hirth, G. Rheology of the Fluid Oversaturated Fault Zones at the Brittle-Plastic Transition. *Journal of Geophysical Research: Solid Earth*, 126(2), Feb. 2021. doi: 10.1029/2020jb020804.

Okudaira, T., Shigematsu, N., Harigane, Y., and Yoshida, K. Grain size reduction due to fracturing and subsequent grain-size-sensitive creep in a lower crustal shear zone in the presence of a CO2-bearing fluid. *Journal of Structural Geology*, 95:171–187, Feb. 2017. doi: 10.1016/j.jsg.2016.11.001.

Oliot, E., Goncalves, P., Schulmann, K., Marquer, D., and Lexa, O. Mid-crustal shear zone formation in granitic rocks: Constraints from quantitative textural and crystallographic preferred orientations analyses. *Tectonophysics*, 612–613:63–80, Feb. 2014. doi: 10.1016/j.tecto.2013.11.032.

Oskin, M., Perg, L., Shelef, E., Strane, M., Gurney, E., Singer, B., and Zhang, X. Elevated shear zone loading rate during an earthquake cluster in eastern California. *Geology*, 36(6):507, 2008. doi: 10.1130/g24814a.1.

Palazzin, G., Raimbourg, H., Stünitz, H., Heilbronner, R., Neufeld, K., and Précigout, J. Evolution in H2O contents during deformation of polycrystalline quartz: An experimental study. *Journal of Structural Geology*, 114:95–110, Sept. 2018. doi: 10.1016/j.jsg.2018.05.021.

Passchier, C. W. and Trouw, R. A. J. *Microtectonics*. Springer Berlin Heidelberg, 2nd edition, 2005. doi: 10.1007/3-540-29359-0.

Peacock, J. M. Temperature and Leaf Growth in Four Grass Species. *The Journal of Applied Ecology*, 13(1):225, Apr. 1976. doi: 10.2307/2401942.

Phelps, P. R., Lee, C.-T. A., and Morton, D. M. Episodes of fast crystal growth in pegmatites. *Nature Communications*, 11(1), Oct. 2020. doi: 10.1038/s41467-020-18806-w.

Phillips, G. N. and Powell, R. Formation of gold deposits: a metamorphic devolatilization model. *Journal of Metamorphic Geology*, 28(6):689–718, July 2010. doi: 10.1111/j.1525-1314.2010.00887.x.

Platt, J. and Behr, W. Lithospheric shear zones as constant stress experiments. *Geology*, 39(2):127–130, Feb. 2011. doi: 10.1130/g31561.1.

Platt, J. P. Rheology of two-phase systems: A microphysical and observational approach. *Journal of Structural Geology*, 77: 213–227, Aug. 2015. doi: 10.1016/j.jsg.2015.05.003.

Pongrac, P., Jeřábek, P., Stünitz, H., Raimbourg, H., Heilbronner, R., Racek, M., and Nègre, L. Mechanical properties and recrystallization of quartz in presence of H2O: Combination of cracking, subgrain rotation and dissolution-precipitation processes. *Journal of Structural Geology*, 160:104630, July 2022. doi: 10.1016/j.jsg.2022.104630.

Price, N. A., Johnson, S. E., Gerbi, C. C., and West, D. P. Identifying deformed pseudotachylyte and its influence on the strength and evolution of a crustal shear zone at the base of the seismogenic zone. *Tectonophysics*, 518–521:63–83, Jan. 2012. doi: 10.1016/j.tecto.2011.11.011.

Précigout, J., Prigent, C., Palasse, L., and Pochon, A. Water pumping in mantle shear zones. *Nature Communications*, 8(1), June 2017. doi: 10.1038/ncomms15736.

Précigout, J., Stünitz, H., and Villeneuve, J. Excess water storage induced by viscous strain localization during high-pressure shear experiment. *Scientific Reports*, 9(1), Mar. 2019. doi: 10.1038/s41598-019-40020-y.

Pucci, S., De Martini, P., and Pantosti, D. Preliminary slip rate estimates for the Düzce segment of the North Anatolian Fault Zone from offset geomorphic markers. *Geomorphology*, 97(3–4): 538–554, May 2008. doi: 10.1016/j.geomorph.2007.09.002.

Putnis, A. and Austrheim, H. Fluid-induced processes: metasomatism and metamorphism. *Geofluids*, 10(1–2):254–269, May 2010. doi: 10.1111/j.1468-8123.2010.00285.x.

Rhys, D. A., Lewis, P. D., and Rowland, J. V. *Structural controls on ore localization in epithermal gold-silver deposits: A mineral systems approach*, page 83–145. Society of Economic Geologists, 2020. doi: 10.5382/rev.21.03.

Rolandone, F., Bürgmann, R., and Nadeau, R. M. The evolution of the seismic-aseismic transition during the earthquake cycle:

Constraints from the time-dependent depth distribution of aftershocks. *Geophysical Research Letters*, 31(23), Dec. 2004. doi: 10.1029/2004gl021379.

Rowe, C. D. and Griffith, W. A. Do faults preserve a record of seismic slip: A second opinion. *Journal of Structural Geology*, 78:1–26, Sept. 2015. doi: 10.1016/j.jsg.2015.06.006.

Rutter, E. H. and Brodie, K. H. The role of tectonic grain size reduction in the rheological stratification of the lithosphere. *Geologische Rundschau*, 77(1):295–307, Feb. 1988. doi: 10.1007/bf01848691.

Salisbury, J. B., Arrowsmith, J. R., Brown, N., Rockwell, T., Akciz, S., and Ludwig, L. G. The Age and Origin of Small Offsets at Van Matre Ranch along the San Andreas Fault in the Carrizo Plain, California. *Bulletin of the Seismological Society of America*, 108 (2):639–653, Jan. 2018. doi: 10.1785/0120170162.

Sanchez-Alfaro, P., Reich, M., Driesner, T., Cembrano, J., Arancibia, G., Pérez-Flores, P., Heinrich, C. A., Rowland, J., Tardani, D., Lange, D., and Campos, E. The optimal windows for seismically-enhanced gold precipitation in the epithermal environment. *Ore Geology Reviews*, 79:463–473, Dec. 2016. doi: 10.1016/j.oregeorev.2016.06.005.

Sanematsu, K., Watanabe, K., Duncan, R., and Izawa, E. THE HISTORY OF VEIN FORMATION DETERMINED BY 40Ar/39Ar DATING OF ADULARIA IN THE HOSEN-1 VEIN AT THE HISHIKARI EPITHERMAL GOLD DEPOSIT, JAPAN. *Economic Geology*, 101(3):685–698, May 2006. doi: 10.2113/gsecongeo.101.3.685.

Schmidt, W. L. and Platt, J. P. Stress, microstructure, and deformation mechanisms during subduction underplating at the depth of tremor and slow slip, Franciscan Complex, northern California. *Journal of Structural Geology*, 154:104469, Jan. 2022. doi: 10.1016/j.jsg.2021.104469.

Scholz, C. H. The brittle-plastic transition and the depth of seismic faulting. *Geologische Rundschau*, 77(1):319–328, Feb. 1988. doi: 10.1007/bf01848693.

Sibson, R. Shear zone models, heat flow, and the depth distribution of earthquakes in the continental crust of the United States. *Bulletin of the Seismological Society of America*, 72: 151–163, 1982.

Sibson, R. H. Fault rocks and fault mechanisms. *Journal of the Geological Society*, 133(3):191–213, Mar. 1977. doi: 10.1144/gsjgs.133.3.0191.

Sibson, R. H. Earthquake rupturing as a mineralizing agent in hydrothermal systems. *Geology*, 15(8):701, 1987. doi: 10.1130/0091-7613(1987)15<701:eraama>2.0.co;2.

Sibson, R. H., Robert, F., and Poulsen, K. H. High-angle reverse faults, fluid-pressure cycling, and mesothermal gold-quartz deposits. *Geology*, 16(6):551, 1988. doi: 10.1130/0091-7613(1988)016<0551:harffp>2.3.co;2.

Singleton, J. S., Rahl, J. M., and Befus, K. S. Rheology of a coaxial shear zone in the Virginia Blue Ridge: Wet quartzite dislocation creep at 250–280 °C. *Journal of Structural Geology*, 140:104109, Nov. 2020. doi: 10.1016/j.jsg.2020.104109.

Song, W. J., Johnson, S. E., and Gerbi, C. C. Quartz fluid inclusion abundance and off-fault damage in a deeply exhumed, strike-slip, seismogenic fault. *Journal of Structural Geology*, 139: 104118, Oct. 2020. doi: 10.1016/j.jsg.2020.104118.

Spruzeniece, L. and Piazolo, S. Strain localization in brittle–ductile shear zones: fluid-abundant vs. fluid-limited conditions (an example from Wyangala area, Australia). *Solid Earth*, 6(3):881–901, July 2015. doi: 10.5194/se-6-881-2015.

Strozewski, B., Sly, M. K., Flores, K. M., and Skemer, P. Viscoplastic Rheology of α-Quartz Investigated by Nanoindentation. *Journal of Geophysical Research: Solid Earth*, 126(9), Sept. 2021. doi: 10.1029/2021jb022229.

Stünitz, H. and Tullis, J. Weakening and strain localization produced by syn-deformational reaction of plagioclase. *International Journal of Earth Sciences*, 90(1):136–148, Dec. 2000. doi: 10.1007/s005310000148.

Stünitz, H., Thust, A., Heilbronner, R., Behrens, H., Kilian, R., Tarantola, A., and Fitz Gerald, J. D. Water redistribution in experimentally deformed natural milky quartz single crystals—Implications for H2O-weakening processes. *Journal of Geophysical Research: Solid Earth*, 122(2):866–894, Feb. 2017. doi: 10.1002/2016jb013533.

Sullivan, W. A. and O'Hara, E. J. A natural example of brittle-to-viscous strain localization under constant-stress conditions: a case study of the Kellyland fault zone, Maine, USA. *Geological Magazine*, 159(3):421–440, Nov. 2021. doi: 10.1017/s0016756821001035.

Tullis, J. and Yund, R. A. Dynamic recrystallization of feldspar: A mechanism for ductile shear zone formation. *Geology*, 13(4):238, 1985. doi: 10.1130/0091-7613(1985)13<238:drofam>2.0.co;2.

Tullis, J. and Yund, R. A. Hydrolytic weakening of quartz aggregates: The effects of water and pressure on recovery. *Geophysical Research Letters*, 16(11):1343–1346, Nov. 1989. doi: 10.1029/gl016i011p01343.

van Haren, J. L., Ague, J. J., and Rye, D. M. Oxygen isotope record of fluid infiltration and mass transfer during regional metamorphism of pelitic schist, Connecticut, USA. *Geochimica et Cosmochimica Acta*, 60(18):3487–3504, Sept. 1996. doi: 10.1016/0016-7037(96)00182-2.

Vignaroli, G., Rossetti, F., Petracchini, L., Argante, V., Bernasconi, S. M., Brilli, M., Giustini, F., Yu, T.-L., Shen, C.-C., and Soligo, M. Middle Pleistocene fluid infiltration with 10–15 ka recurrence within the seismic cycle of the active Monte Morrone Fault System (central Apennines, Italy). *Tectonophysics*, 827:229269, Mar. 2022. doi: 10.1016/j.tecto.2022.229269.

Wallis, D., Lloyd, G. E., and Hansen, L. N. The role of strain hardening in the transition from dislocation-mediated to frictional deformation of marbles within the Karakoram Fault Zone, NW India. *Journal of Structural Geology*, 107:25–37, Feb. 2018. doi: 10.1016/j.jsg.2017.11.008.

Weatherley, D. K. and Henley, R. W. Flash vaporization during earthquakes evidenced by gold deposits. *Nature Geoscience*, 6 (4):294–298, Mar. 2013. doi: 10.1038/ngeo1759.

Weldon, R., Scharer, K., Fumal, T., and Biasi, G. Wrightwood and the earthquake cycle: What a long recurrence record tells us about how faults work. *GSA Today*, 14(9):4, 2004. doi: 10.1130/1052-5173(2004)014<4:watecw>2.0.co;2.

Wesnousky, S. G. Seismological and structural evolution of strike-slip faults. *Nature*, 335(6188):340–343, Sept. 1988. doi: 10.1038/335340a0.

Wesnousky, S. G., Barron, A. D., Briggs, R. W., Caskey, S. J., Kumar, S., and Owen, L. Paleoseismic transect across the northern Great Basin. *Journal of Geophysical Research: Solid Earth*, 110 (B5), May 2005. doi: 10.1029/2004jb003283.

White, S. Geological significance of recovery and recrystallization processes in quartz. *Tectonophysics*, 39(1–3):143–170, Apr. 1977. doi: 10.1016/0040-1951(77)90093-2.

White, S. H. and Knipe, R. J. Transformation- and reaction-enhanced ductility in rocks. *Journal of the Geological Society*, 135(5):513–516, Sept. 1978. doi: 10.1144/gsjgs.135.5.0513.

Whitehead, B. A., Harris, C., and Sloan, R. A. Deep infiltration of surface water during deformation? Evidence from a low-δ18O shear zone at Koegel Fontein, Namaqualand,

South Africa. *Lithos*, 366–367:105562, Aug. 2020. doi: 10.1016/j.lithos.2020.105562.

Williams, R. T. and Fagereng, A. The Role of Quartz Cementation in the Seismic Cycle: A Critical Review. *Reviews of Geophysics*, 60 (1), Mar. 2022. doi: 10.1029/2021rg000768.

Wintsch, R. P. and Yeh, M.-W. Oscillating brittle and viscous behavior through the earthquake cycle in the Red River Shear Zone: Monitoring flips between reaction and textural softening and hardening. *Tectonophysics*, 587:46–62, Mar. 2013. doi: 10.1016/j.tecto.2012.09.019.

Woodcock, N. H., Dickson, J. A. D., and Tarasewicz, J. P. T. Transient permeability and reseal hardening in fault zones: evidence from dilation breccia textures. *Geological Society, London, Special Publications*, 270(1):43–53, Jan. 2007. doi: 10.1144/gsl.sp.2007.270.01.03.

Zinke, R., Dolan, J. F., Rhodes, E. J., Van Dissen, R., and McGuire, C. P. Highly Variable Latest Pleistocene-Holocene Incremental Slip Rates on the Awatere Fault at Saxton River, South Island, New Zealand, Revealed by Lidar Mapping and Luminescence Dating. *Geophysical Research Letters*, 44(22), Nov. 2017. doi: 10.1002/2017gl075048.

Zinke, R., Dolan, J. F., Rhodes, E. J., Van Dissen, R., McGuire, C. P., Hatem, A. E., Brown, N. D., and Langridge, R. M. Multimillennial Incremental Slip Rate Variability of the Clarence Fault at the Tophouse Road Site, Marlborough Fault System, New Zealand. *Geophysical Research Letters*, 46(2):717–725, Jan. 2019. doi: 10.1029/2018gl080688.

Zinke, R., Dolan, J. F., Rhodes, E. J., Van Dissen, R. J., Hatem, A. E., McGuire, C. P., Brown, N. D., and Grenader, J. R. Latest Pleistocene–Holocene Incremental Slip Rates of the Wairau Fault: Implications for Long-Distance and Long-Term Coordination of Faulting Between North and South Island, New Zealand. *Geochemistry, Geophysics, Geosystems*, 22(9), Sept. 2021. doi: 10.1029/2021gc009656.